Erasmus University Medical Center, department of radiotherapy

-

Delft University of Technology

FLASH optimisation in clinical IMPT treatment planning

optimisation and evaluation of stereotactic lung treatment plans with proton transmission beams

MSc Thesis

Author:
J. Groen
4618378

Supervisor Erasmus University Medical Center:
Dr S.J.M. Habraken

Supervisor Delft University of Technology:
Dr Ir. D. Lathouwers

July 1, 2020

Abstract

Radiotherapy (RT) is an important modality in treatment against cancer. Developments in this modality are necessary for improvement of patient complications and survival. Aside from fractionation and precise irradiation, FLASH radiotherapy could be a third way to significantly increase the therapeutic window of radiotherapy.

The FLASH effect is a biological, healthy tissue sparing effect that is found in tissue that receive a high dose (>10 Gy) within a very-short irradiation time (<100 ms). Although the mechanics behind the FLASH effect remain unknown, it is found to benefit a large variety of tissues and organs. Nevertheless, FLASH-RT still lacks clinical translation and implementation of FLASH irradiation is limited by current technology. However, the extremely high dose rates required for FLASH can readily be achieved using cyclotron accelerated proton transmission beams. Cancer patients with small lung tumours are a preferred starting point for clinical translation of FLASH because (i) transmission beams are of special benefit for lung tumours since they mitigate for range uncertainties and contain a sharp lateral penumbra, (ii) high doses are required for the FLASH effect to occur and hypofractionation is not uncommon for lung patients, and (iii) the very-short irradiation times and high doses in combination with gating allow smaller treatment margins for moving tumours.

In this study, we took a first step towards intensity modulated proton therapy (IMPT) with FLASH treatment plan optimisation by (i) investigating the most delivery-time effective way to irradiate a field, (ii) proposing an optimisation method to maximise FLASH within a treatment plan, and (iii) analysing and evaluating FLASH treatment plans.

Because increased pencil-beam (spot) separation showed to benefit the pencil-beam scanning (PBS) delivery time of a field, spot overlap minimisation was proposed as optimisation method for FLASH. Treatment plans using 3, 5 and 7 transmission beams were generated with and without FLASH optimisation for 6 small lung tumour patients. Although spot overlap minimisation does occasionally improve delivery time for a limited number of beam angles, the overall treatment plan does not benefit from the optimisation. Therefore, spot overlap minimisation cannot be used for FLASH optimisation in clinical IMPT treatment planning. Recommendations for future research include optimisation on PBS delivery time and PBS pattern optimisation.

Preface

This report is written within the framework of a master thesis project conducted by Jort Groen, master student Biomedical engineering at the Delft University of Technology, The Netherlands. This project is commissioned by the Erasmus Medical Centre, Rotterdam, The Netherlands. "The Erasmus MC encompasses a full spectrum of clinical services, including those provided by two specialist units operating under the Erasmus MC umbrella: the Erasmus MC Sophia Children's Hospital and the Erasmus MC Cancer Institute. Both have unique reputations of their own in the world of university hospitals." [1].

I would like to thank everybody, who in his/her way contributed to this study. In particular, I would like to thank my daily supervisor Steven Habraken, who was closely involved in my research and of big help writing this thesis. I would like to thank Danny Lathouwers for his guidance during the project and critical feedback on my writing. Finally, I would like to thank Sebastiaan Breedveld and Mischa Hoogeman for coaching me weekly and helping me with technical problems.

Table of Contents

1

Introduction

1.1. Radiotherapy

Treatment of cancer often involves a combination of three main modalities. Surgery for local tumours, radiotherapy for local-regional control and chemotherapy for systemic disease. For systemic treatment, additional new modalities such as immunotherapy and hormonotherapy are also used nowadays. About half of all cancer patients receive radiotherapy as part of their treatment. In radiotherapy, ionising radiation is used to cause DNA damage in tumour cells that results in their direct cell death or reduced cell-growth. Radiotherapy is used as a stand-alone modality or in combined treatment where it is applied after surgery to kill remaining tumour cells left in the target area. In this thesis, we focus on external beam radiotherapy that uses one or more beams of radiation, targeted at the tumour from outside of the patient's body.

The side effect of radiotherapy, that is, healthy tissue toxicity, can result in deterministic and stochastic effects. Stochastic effects are found as secondary tumours, occurring years after treatment. Deterministic effects can be separated in early and late toxicities from which late toxicities are treatment-dose limiting. Clinical examples of late toxicities are: Impact on cognitive function after brain irradiation, dry mouth and swallowing problems after head and neck treatment, and reduced lung function after irradiation of lung tumours and lung metastasis.

Given the large number of RT treatments, further development of this modality is crucial for the improvement of cancer patient care as a whole. Developments in radiotherapy often aim to minimise its side effects. Since tumour cells are intrinsically more radiosensitive compared to healthy cells, there is a difference between the tumour control probability (TCP) and normal tissue complication probability (NTCP) at any given dose. The space between TCP and NTCP is called the therapeutic window. This therapeutic window is significantly increased after introduction of fractionation, medical imaging in combination with high-precision irradiation techniques, and soon to come, FLASH.

In fractionation, the planned treatment dose is divided into multiple fractions, often given on a day-to-day basis. In the period between these fractions, healthy tissue has time to (partially) repair the DNA damage, inflicted by the radiation. Since tumorous cells are less capable of DNA self-repair, a differential effect occurs that grows during treatment as more fractions are given. This differential effect enlarges the therapeutic window. However, not all tumour cells are radiosensitive, making the differential effect of fractionation less pronounced, or worse, completely absent.

The effect of fractionation can be investigated using the linear-quadratic model that describes the cell survival fraction as function of delivered dose. Using this model, the biologically effective dose (BED) is derived as an indication of the dose that a tissue experiences as function of number of fractions, dose per fraction and tissue radiosensitivity.

In any case, it is important to spare healthy tissue as much as possible. Precise volume optimisation enables this by optimising multiple beam angles and shapes such that healthy tissue doses are minimised while maintaining sufficient tumour coverage. Unfortunately, tumours infiltrate normal tissue, making it unavoidable to also irradiate healthy tissue in these areas. Furthermore, day-to-day changes in patient anatomy, patient alignment errors, irradiation inaccuracy and patient motion during irradiation introduce uncertainties. For this, treatment margins are introduced that expand the target area to ensure tumour coverage and therewith tumour control. New technologies such as online imaging (CBCT, MRI-linac) and more precise techniques (Cyberknife, proton therapy) make radiotherapy more accurate than ever, allowing margins to be smaller and smaller.

1.2. Proton radiotherapy

Traditional external beam radiotherapy is typically done using electrons and photons (X-rays). As a photon beam travels through a patient's body, energy is deposited along its path, following a defined curve. At first, the energy deposited, and therewith dose, is increasing as the photons travel deeper inside the patient. At a certain depth, the relative energy deposition reaches its maximum in the shape of a peak. After this peak, the energy deposited along the beam path decreases again until the beam leaves the patient. Because the energy range is limited for modern clinical accelerators, the photon peak occurs close to the skin. Therefore, the tumour is almost always irradiated using the tail of the curve, leaving the dose peak being delivered in healthy tissue. The doses delivered to healthy tissue in front of the tumour are called entry doses. The doses delivered to healthy tissue behind the tumour are called exit doses.

Because of the mass and charge of a proton, the energy deposition curve of a proton beam is far more peaked. This characteristic pointy peak in the proton dose-deposition curve is called the 'Bragg peak'. By changing the initial energy of the protons, the Bragg peak occurs at different depths. This effect is used to aim the dose peak inside of the tumour. Having significantly less entry and zero exit doses, proton therapy allows for better sparing of healthy tissue compared to photon therapy. By delivering protons with a defined energy range, a dose plateau is created that is used to cover the tumour in longitudinal direction. Tumour shape in lateral direction is covered by the shape of the irradiating beam. Occasionally, very high energies are used that do not contain a Bragg peak inside the patient anymore. In this case, irradiation is said to be done using so called 'transmission beams'.

One of the ways to cover lateral tumour shape is by using pencil-beam scanning (PBS). Here, the beam shape is defined as a composition of smaller 'pencil-beams' (spots). Using a variable spot pattern and modulating spot intensities, both varied for different energies/depths, any tumour volume can accurately be irradiated. Similar to photon therapy, multiple beam angles and shapes are used to irradiate the target volume while sparing healthy tissue and avoiding organs at risk (OARs) as much as possible. Optimisation of beam shapes and angles is done using treatment planning software. Based on a CT scan of the patient that contains delineated OARs and targets, the dose distribution is optimised such that the tumour control probability is sufficiently high and healthy tissue doses are clinically acceptable.

While in many cases proton therapy is preferable over photon therapy, the costs of a proton treatment site are significantly larger than that of photons. Although a modern particle accelerator is relatively compact and cost effective, the gantry, necessary for guiding the proton beam over different angles, is colossal and expensive. New developments are made into creating compact proton irradiation systems to make implementation of proton therapy in existing hospitals more accessible. Nevertheless, as of May

2020, the number of proton therapy institutions around the world is 92 and vastly growing [2]. In the Netherlands, three treatment centres are in use. Patients from the Erasmus Medical Centre are referred to Holland PTC for proton therapy. Holland PTC is an independent proton therapy centre, founded by the Erasmus MC, LUMC and TU Delft, established with the purpose of both treatment of patients and research. In Holland PTC, 3 treatment rooms are available using the Varian ProBeam 360 delivery system. The centre has two general treatment gantries, an eye treatment room, and a dedicated research room.

1.3. FLASH radiotherapy

In addition to fractionation and precise irradiating techniques, a new biological effect has been (re-) discovered that could potentially widen the therapeutic window significantly. This effect, called 'FLASH', is found in high dose volumes, irradiated in very-short irradiation times using very-high dose rates. The current consensus for FLASH therapy is delivering doses larger than 10Gy, within irradiation times lower than 100 ms and using dose rates larger than 100 Gy/s. FLASH irradiation enables healthy tissue to tolerate higher doses. The FLASH effect was found for a variety of different tissues and organs both in vitro and *in vivo* such as intestine [3], [4], brain [5]-[7], skin [8] and lung [9], [10]. Furthermore, recently, the first human patient was treated using FLASH-RT [11].

Although many studies have found the presence of a FLASH effect, the biological mechanisms behind the effect are not well-understood. Possible explanations for FLASH mechanics include radiolytic oxygen depletion (ROD), changes in redox metabolism, circulating immune cell sparing and differences in chromatin remodelling. Although the relation between additional tissue sparing and oxygen depletion using high dose-rates has been known since the 1960s and 1970s [12]-[18], and the ROD theory is in agreement to the in vitro studies, it does not seem to accurately describe the *in vivo* results of FLASH [19]. Therefore, it is likely that other (biological) mechanisms or combination of effects play a role in the explanation of FLASH. Research on the mechanics of FLASH is currently practiced but all theories still need to be tested further. Further background on FLASH can be found in the literature study "How to optimise FLASH in clinical IMPT treatment planning" in appendix D.

1.3.1. FLASH proton therapy

Most FLASH studies are performed using electron irradiation, delivered using a custom linear accelerator (linac) [4]-[9], [11], [20], [21]. Three FLASH studies were performed using protons [3], [10], [22] of which two found a FLASH effect [3], [10]. Therapeutic protons are usually accelerated using cyclotrons or synchrotrons. However, only cyclotrons are capable of achieving high enough (mean) dose-rates needed for FLASH. Because beamline transport is more efficient at higher energies, FLASH compatible dose-rates are obtained using cyclotrons when operating at maximum energy, often about 250 MeV.

However, there are differences between FLASH cyclotron and linac dose delivery and even more so between future FLASH IMPT and the currently done FLASH irradiations. First of all, cyclotron proton beams are relatively continuous, delivering a FLASH dose-rate of about 800-1000 Gy/s at the centre of the (pencil) beam. This is in contrast with the mostly used FLASH linac electron irradiation that has a pulsated delivery, with a frequency of 100-150 Hz and contains an instantaneous dose-rate of millions of Gy/s within pulse. Secondly, in clinical proton treatment, more than one beam angles are used, each intensity modulated using pencil-beam scanning. Up to today, all FLASH irradiations done have only used single beams without intensity modulation. Stereotactic dose delivery and beam modulation introduce tissue revisits due to beam overlap between beams and pencil beam (spot) overlap within beams. The influence of beam- and spot overlap on FLASH is currently unknown. FLASH proton irradiation is also different from conventional IMPT, the high energies needed to achieve FLASH compatible mean dose-rates inside a beam result in the Bragg peak being shifted out of the patient and thereby nullifies the main advantage of protons. Nevertheless, clinical treatment plans using high-energy

proton transmission beams are possible and can even be advantageous over stereotactic photon irradiation in treatment of lung tumours. This is due to the fact that transmission beams mitigate range uncertainties and reduce movement uncertainties such as respiratory induced motion, a common problem when treating lung tumours [23].

1.3.2. The FLASH triangle

Because the mechanics behind FLASH remain undiscovered, modelling of the effect is impossible. Furthermore, current FLASH studies show a large variety in irradiation parameters such as instantaneous- and mean dose-rates, delivery-time, delivered dose and field size. Additionally, several of these parameters are often not reported. Therefore, direct optimisation on FLASH is not possible. Hence, we approach FLASH treatment planning from a clinical-physics perspective.

Although optimisation on FLASH itself is infeasible, it is possible to evaluate on FLASH indicators that have previously been linked to a FLASH effect observation. These indicators include: High dose, low irradiation time and high dose-rate [19]. A treatment plan optimisation that shows improvement on these evaluations is likely to increase the FLASH potential. However, in radiotherapy treatment planning, the FLASH indicators are not independent. Dose, irradiation time and dose rate are intertwined as followed:

$$Dose\ rate = \frac{Dose}{irradiation\ time} \tag{1}$$

In a conventional treatment plan, optimisation is aimed at the dose distribution. Creating a FLASH optimised plan includes, aside from achieving a clinically acceptable dose distribution, minimisation of irradiation time and maximisation of dose rates. These optimisation criteria are conflicting. For example, reduced irradiation time might sacrifice conformity around the target, often desired in physical dose distributions. The intrinsic trade-of between dose, irradiation time and dose-rate is visualised in figure 1 as the so-called “FLASH triangle”.

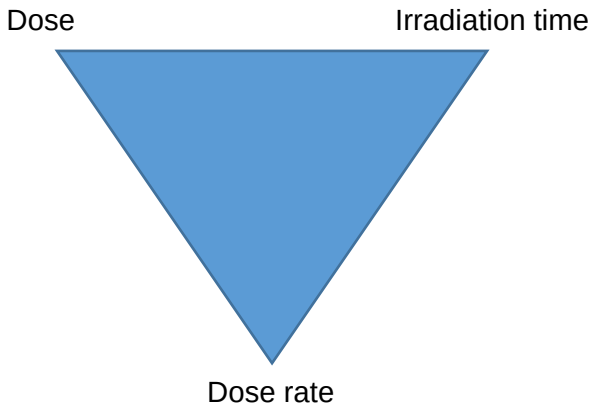

Figure 1: The FLASH triangle contains dose, irradiation time and dose-rate. Optimisation on one of the three points results in a trade-off on the others. Dose and irradiation time are conflicting optimisation objectives. Dose-rate can be improved when optimising the others.

1.4. Problem definition

Even though radiotherapy is more precise than ever, its side effect, that is, healthy tissue toxicity, remains unavoidable due to (i) entry doses, (ii) tumour infiltration in healthy tissue and (iii) treatment margins that are necessary to assure tumour control. The side effects often limit the capabilities of radiotherapy. In some cases, severe irradiation side effects occur in patients and impacts quality of life after treatment. In other cases, dose-tolerance of healthy tissue, limits the ability to adequately irradiate tumours. The FLASH effect potentially enlarges the therapeutic window and offers perspective in both cases.

Although the effect has been found repeatedly both in vitro and *in vivo*, and the number of studies is growing at an increasing rate, FLASH currently lacks clinical translation. Nevertheless, FLASH dose rates are readily available for protons. Besides, the true clinical value of FLASH can only be investigated in clinical setting. This can be done by generating (FLASH) treatment plans within clinical dose constraints, potentially combined with dose-rate escalation studies in which the dose rate in palliative setting is gradually increased to investigate whether the treatment is safe for patients.

Since the FLASH effect has previously been found for proton irradiation and current cyclotrons are technically able to deliver the very-high dose rates when operating at maximum energy, transmission beam IMPT is a logical first step to investigate the clinical added value of FLASH. However, IMPT irradiation include tissue revisits both between beams as result of beam overlap, and within beams as result of spot overlap, the presence of a FLASH effect in IMPT treatment plans is not trivial. Furthermore, the absence of knowledge about the mechanics of FLASH and the uncertainties about the various FLASH irradiation parameters makes direct optimisation of FLASH inside a treatment plan impossible. This raises the following question: “How can FLASH be optimised in clinical IMPT treatment planning?”.

Two studies already compared different IMPT treatment plan strategies for FLASH radiotherapy. Van Marlen *et al.* already investigated dose-rate distributions and delivery times for FLASH proton transmission beam plans as an alternative for stereotactic lung photon-irradiation. For 7 patients, treatment plans were created using 10 largely noncoplanar transmission beams. These plans were compared on dose to volumetric modulated arc therapy (VMAT) plans and evaluated on FLASH by assessing dose rate and irradiation time. It was found that FLASH potential within a treatment plan increases with spot intensity [24]. Van de Water *et al.* compared different IMPT treatment plan approaches and delivery methods for four head-and-neck patients. It was concluded that FLASH compatible dose rates were best achieved when using increased spot intensities, spot-reduced planning, hypofractionation and arc-shoot-through (transmission beam) plans [25].

1.5. This thesis

Although different treatment planning strategies were evaluated on FLASH potential, FLASH treatment plan optimisation has not yet been done. In this study, we attempt to set up a FLASH treatment planning system from a clinical physics perspective, using small lung tumours as paradigm. Here, lung patients are used since (i) FLASH compatible dose rates are readily available using proton transmission beams that have a special benefit for lung tumours, and (ii) the FLASH effect was previously found to benefit long tissue. A treatment plan is considered a FLASH compatible treatment plan when all or most of the dose delivery is done within the currently set FLASH constraints, i.e. doses > 10 Gy, irradiation times < 100 ms and dose rates > 100 Gy/s. Optimisation on FLASH therefore aims to maximise the volume that is irradiated within these constraints.

We will set up the FLASH treatment planning system by first, modelling dose delivery for a circular field, determining the influence of spot separation and number of spots on delivery time, and its dependence on field size and target dose. From this, the best way to irradiate a field with the lowest delivery time possible is determined. Based on these results, a FLASH optimisation method is proposed and implemented in a treatment planning system. Hereafter, transmission beam treatment plans with and without FLASH optimisation are generated for 6 small lung tumour patients. These plans are then evaluated on dose, irradiation time and dose rate. Furthermore, the influence of the newly proposed optimisation method is identified and evaluated.

For the treatment plan optimisation, the in-house created iCycle treatment planning software is used [26]. For both optimisation and analysis, parameters are used of the Varian ProBeam 360 delivery system with an upgraded beam current to 400 nA at the snout when operating at maximum commissioned cyclotron energy (244 MeV). Since this study is focussed on proof of principle, robustness planning is not applied. Thorough clinical validation of the treatment plans is also out of scope.

In chapter 2 we discuss the methods, describing how the artificial fields are modelled, optimised and analysed to determine the best way to deliver a field such that the delivery time is the lowest. We will clarify what patients are included in the study, how treatment planning is performed, how the treatment plans are evaluated on FLASH and our proposed method for treatment plan optimisation on FLASH. In chapter 3, ‘results’, we start with analysing the modelled fields, determine the best way to define a field such that the delivery time is minimal, therewith reason the proposed FLASH optimisation method and state a rough indication for the maximum field size within FLASH constraints. Hereafter, evaluation of the three FLASH indicators is performed on the treatment plans that are generated. The results and methods of this study are discussed in chapter 4. At last, the research was concluded in chapter 5 together with an outlook in chapter 6.

2 Methods

2.1. Treatment planning dose optimisation

Conventionally, treatment plans are optimised on dose distribution. In this study, we make use of the Erasmus MC in-house developed treatment planning software 'iCycle' [26]. iCycle is superior to other treatment planning systems due to its prioritised optimisation and the ability to create hard constraints. Because of this, wish lists are used that generalises to a patient group versus manual tweaking of a cost function per patient as required in other treatment planning systems. This allows for a better definition of clinical preferences as input to the optimisation and thereby creates treatment plans of exceptional quality while maintaining high generalisation over patients. The prioritised optimisation and constraints functionality is of special benefit for FLASH treatment planning because optimisation on irradiation time and dose rates will counteract dose goals. Using prioritised optimisation, it is possible to manage which goals can be compromised on for the optimisation of FLASH. Furthermore, while optimising on FLASH, the constraints functionality can still ensure that (i) target dose remains achieved and (ii) OAR clinical constraints are not violated.

In the iCycle software package, a 'wish list' is defined containing all optimisation objectives and constraints. These objectives and constraints are linked to structures that are defined using the delineated volumes. The objectives are optimised one by one according to the order of their assigned priority. In most cases, objectives and constraints are optimised either linear (based on the maximum dose) or using the mean dose. Treatment plan optimisation is done by first selecting a set of spots (pencil beams) for all defined beam angles.
Secondly, for every spot, the dose is determined for each voxel within all defined structures after delivery of 1 Giga-protons. These dose points are stored in a matrix denoted as 'A'. Since dose-calculation is computationally expensive, matrix 'A', is used for objective optimisation. Here, the dose in Gy per voxel, saved vector '$\bar{d}$' is determined by multiplying the matrix 'A' with the spot weights vector '$\bar{x}$', that contains the amount of Giga-protons that are delivered per spot:

$$\bar{d} = A\bar{x} \tag{2}$$

In the third step, the objectives are optimised. For each objective, the spot weights '$\bar{x}$' are optimised such that the dose, defined by equation 2, approaches the defined goal within the objective's target structure and does not violate any of the constraints. This objective optimisation is done for all objectives, ordered, according to priority. This is done for multiple iteration and after each iteration, spots that appear to be insignificant are removed. Finally, the dose is calculated within the entire patient CT and the treatment plan is saved.

2.2. Pencil beam scanning delivery time

It is clear that irradiation time plays an important role in FLASH-RT. However, irradiation time on itself can be defined in various ways. In this study, the pencil-beam scanning delivery time is used as proposed by the Varian FLASHforward consortium. This quantity is determined per voxel and defined as the interval time between the first and last moment a pencil beam delivers dose to this voxel that exceeds 1 cGy. A visual representation of this delivery time definition is given in figure 2.

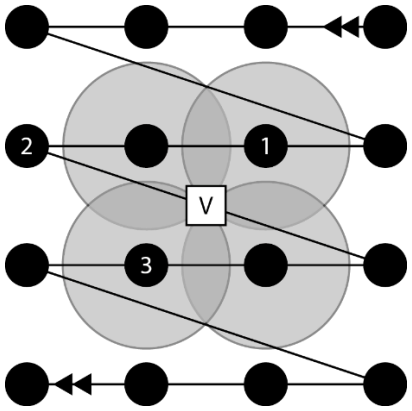

Figure 2: Illustration of pencil beam scanning dose-rate time interval on a rectangular grid for voxel 'V'. During PBS, the first pencil beam delivering a dose exceeding 0.01 Gy at voxel V is denoted by '1'. The last pencil beam contributing more than 0.01 Gy to 'V' is denoted by '3'. Pencil beam 2 does not contribute dose to voxel 'V'. However, since the spot is delivered between the first and last spot that hits 'V', the spot delivery time still contributes to the time interval.

The PBS delivery time is composed out of spot irradiation times and travel times. The irradiation time for a single spot is calculated as followed:

$$T_{spot} = \frac{x \cdot e}{I} \tag{3}$$

where T_{spot} is the spot delivery time in seconds, x is the spot weight in Giga-protons, e is the elementary charge ($1.6 \cdot 10^{-19}\ C$) and I is the beam current (400 nA).

2.3. Modelling of FLASH field delivery

To investigate the optimal irradiation approach for FLASH, that is, delivery of the required dose within minimal delivery time and using maximal dose rates, the dependencies of delivery time within a dose field are investigated i.e. field size, spot separation, PBS delivery time and target dose. For this, a theoretical 2D circular field is considered. This field is irradiated with a target dose using j spots. Given that the field should be irradiated homogeneously and conformally, the spots are uniformly distributed over the field. In figure 3 can be seen how a field with a constant field size is irradiated using different number of spots by varying the spot separation.

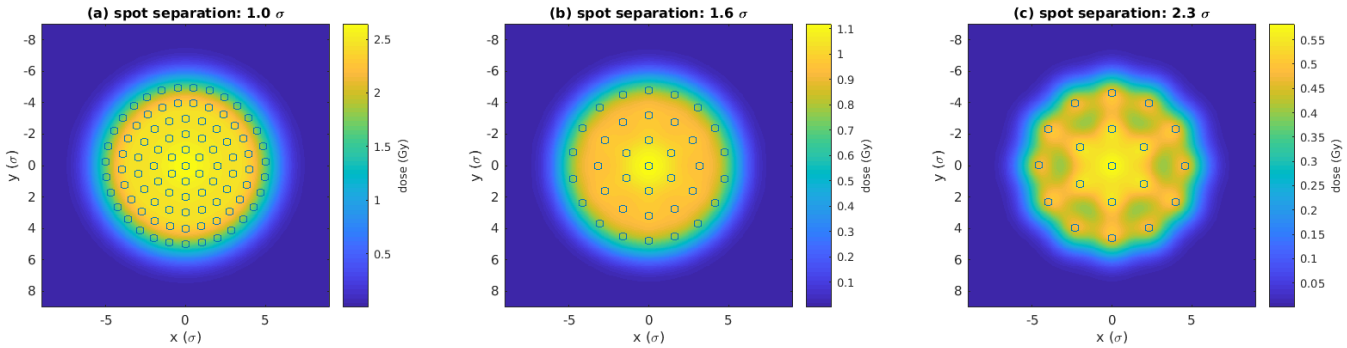

Figure 3: Irradiation of a defined circular field, using varying number of spots by changing the spot separation of (a) 1 standard deviation (σ), (b) 1.6σ and (c) 2.3σ. Larger spot separation results in more fluctuation in dose.

The field is generated using j uniformly distributed spots. The spots are modelled using standard Gaussian distributions with normalised amplitudes. All the individual contributions of the spots to the field are saved in matrix A. Matrix A is then scaled by a factor 'a' to simulate lung tissue dose delivery. Factor 'a' was taken such that matrix A now represents the individual dose contributions of every spot to the field after delivery of 1 Giga-protons. Therefore, the dose inside the field can now be described by equation 2.

As can be seen in figure 3, the field is by default heterogeneous for spot separations larger than 1 std. The spot contributions need to be optimised to create a homogeneous field with an average dose equal to the target dose. This is done in a quadratic way. For this, we evaluate the quadratic difference between the field- and target dose and is rewritten as followed:

$$(\bar{d} - \bar{d}_t)^2 \;=\; (A\bar{x})^2 - 2A\bar{x}\bar{d}_t + \bar{d}_t^2 \;=\; \bar{x}^T A^T A\bar{x} - 2A^T\bar{d}_t\bar{x} + \bar{d}_t^2 \tag{4}$$

Here, $\bar{d}_t$ is the target dose distribution, $\bar{d}$ is the dose distribution inside the field, A is the dose conversion matrix and $\bar{x}$ are the spot weights. The quadratic difference is optimised by varying the spot weights using a quadratic optimiser:

$$\min_x \left\{\frac{1}{2}\bar{x}^T H\bar{x} + \bar{f}^T\bar{x}\right\} \; such\ that\ \{(A\bar{x})_i \leq b\} \tag{5}$$

Where i represents a voxel, b is the maximum allowed dose for any voxel and the following substitutions were used for H and $\bar{f}$:

$H = 2A^T A$;

$\bar{f} \;= (2A^T\bar{d}_t)^T$;

Because the constraint on b results in a upper limit rather than a mean target dose, after optimisation, the spot weights are iteratively scaled such that the mean dose inside the field is equal to the target dose. The initial field size was set have a radius of about 5 (spot) standard deviations. Target doses were varied from 1 to 19 Gy, using a step size of 2 Gy. For every target dose, fields were generated of varying spot separation, ranging from 1 to 2.3 standard deviations. For every field, the field size was varied by turning off spots one-by-one. Each set of spots (sub field) is optimised as described by equation 5 and scaled to have an average sub-field dose equal to the target dose. For every sub field, the PBS delivery time was calculated for row-wise scanning and circular scanning as described in chapter 2.2. For each sub field, the maximum and mean delivery times for both scanning patterns were saved as data points, together

with the sub-field variables (target dose, spot separation and field size). by using the data points mentioned above, the dependence of delivery time will be analysed on both field size, spot separation and dose. Both modelling and evaluation are done using Matlab (version R2017a).

2.4. Patients

Data from 21 early-stage lung cancer or metastasis patients previously treated with photon SBRT at the Erasmus Medical Centre were investigated. To ensure the coherence and consistency of the analysis, patients with atypical anatomies were excluded from the research such as patients with tumours infiltrated in the lung wall and patients with only one lung.

Since transmission beams mitigate for range uncertainties, the delivery uncertainties i.e. systemic and random errors are more similar to that of photon than proton treatment. For this reason, a planning target volume (PTV) was used to account for delivery uncertainties. In all patients, the PTV was created by isotopically expanding the gross tumour volume (GTV). To ensure similar treatment plan conditions, only patients that had a PTV of 5 mm around the GTV were included. Here, 5 mm was chosen for this research so as to reach the maximisation of the number of patients included in the group. In total, 6 patients were included, containing PTV sizes ranging from 5.2 to 31.4 cm^3, shown in table 1. Patient 2 had two tumours, here, the tumour which better fits to the inclusion requirements was chosen as the target.

Table 1: PTV volumes in cubic centimetres of all patients, ranging from 5.2 to 31.4 cc.

#	PTV volume [cc]
1	31.4
2	9.2
3	8.1
4	10.7
5	15.7
6	5.2

Similar to the photon plans, the spinal cord, oesophagus, trachea, main bronchi and ipsilateral lung were included during optimisation as organs-at-risk (OARs) since these organs often result in late deterministic toxicities. All OARs with exception of the lung are serial organs, i.e. high dose at a single point can result in toxicities. The lung is a parallel organ and a local high dose is therefore less critical. For this reason, the clinical constraint on lung dose is determined using the relative lung volume that receives 13 Gy or more (V_{13}). A summary of all OARs and corresponding clinical constraints is given in table 2.

Table 2: Organs at risk clinical constraints. spinal cord, oesophagus, trachea and main bronchi are considered serial organs and therefore constrain the maximum dose. The lung is a parallel organ. Here the constraint is placed on the V_{13} (Volume that receives a dose exceeding 13 Gy).

Organ	Organ type	Volume	Maximum dose [Gy]	Dose per fraction [Gy]
Spinal cord	Serial	Any point	21.6	7.2
Oesophagus	Serial	Any point	31.5	10.5
Trachea	Serial	Any point	36.0	12.0
Main bronchi	Serial	Any point	38.1	12.7
Lung	Parallel	V_{13}	/	<31%

Treatment plans were generated using iCycle as described in chapter 2.1. For every patient, plans containing 3, 5 and 7 equiangular beam angles were generated. The beam set-up was rotated to avoid irradiation of OARS as much as possible. Single energy transmission beams of 244 MeV were applied on all plans. Although the cyclotron of HollandPTC will be able to deliver protons with energies of 250 MeV, 244 MeV is the highest energy currently commissioned and therefore used in this study. It is expected that the differences in percentage depth dose (PDD) and lateral dose profile between pencil beams of 244 and 250 MeV are negligible.

The lung tumours are prescribed 3*17Gy RBE to the 80% isodose. This results in a maximum dose inside the PTV of 125%. In addition to this, an objective is added such that 100% of the PTV volume receives a dose of at least 95% of the target dose. Since the rotation of the cyclotron snout takes seconds, it is assumed that only one beam can be given per fraction within the FLASH delivery time constraint. We therefore use a single beam per fraction approach. Consequentially, using the linear-quadratic model and assuming a tumour radio sensitivity (α/β ratio) of 10, 3*18, 5*13.09 and 7*10.52 Gy are targeted for the 3, 5 and 7-beams plans respectively. After optimisation, treatment plans were normalised such that 95% of the PTV (V_{95}) receives at least 100% of the target dose.

Clinical constraints as given by table 2 are given as a wish-list with which the optimiser finds a solution with exception of the clinical lung constraint since no implementation of V_{13} was in place. To encourage a conformal treatment plan and minimise healthy tissue doses, shells are used around the PTV. These shells are structures that cover the entire patient with exception of the PTV + additional margin. Four shells are used with margins around the PTV of 3, 6, 9 and 20 mm respectively. Objectives are set in the shells that aim at reducing dose. Lower dose objectives are set for shells with a larger margin to force the high-dose area to be conformal to the PTV. The full wish-list can be found in appendix A. The resulting treatment plans are evaluated on dose distribution and dose-volume histograms (DVHs).

2.5. FLASH treatment plan evaluation

An optimal treatment plan delivers the target dose to the PTV while sparing the OARs and other healthy tissue as much as possible. An optimal FLASH treatment plan does so within the FLASH constraints on dose, irradiation time and dose rate. For dose, the common consensus to ensure a FLASH effect is to deliver at least 10 Gy per fraction. Luckily, most OARs are easily avoidable when irradiating using limited number of transmission beams. Because of this, the unavoidable healthy lung tissue dose is the most critical.

To evaluate the doses within OARs and target structures, dose-volume histograms (DVHs) are analysed. Evaluation on dose conformity around the PTV is done by visual inspection of the physical dose distribution. Validation of target dose coverage is done based on the V_{95}, which should receive at least 100% of the target dose. Treatment plans are validated on the PBS delivery time using delivery-time distributions and delivery-time-volume histograms (DTVHs). Because a FLASH effect is expected for only higher doses, DTVHs are made using different dose thresholds of 0.01 and 10 Gy. Both the dose and the PBS delivery time within the treatment plan are distributions with varying values. When dividing the dose at a voxel by its corresponding PBS delivery time, the PBS dose rate for that voxel is obtained. Although this does not provide us with any new information, since other FLASH studies evaluate on mean dose rate, these dose rates are reported as well in this study. We evaluate the dose rates within a treatment plan using dose-rate-volume histograms (DRVHs).

2.6. FLASH optimisation

Higher-level optimisations can be done as alternative to optimisation on dose, irradiation time and dose-rate. For example, spot overlap can be minimised. Although no research is performed on the influence of spot (pencil beam) overlap, large amount of overlap, and therewith tissue revisits, will likely decrease FLASH potential. Decreasing spot overlap decreases tissue revisits and is therefore likely to improve FLASH potential. Furthermore, optimisation on spot overlap is a well-defined geometrical problem, not dependent on any of the FLASH parameters which are still unclear and not fully defined.

Spot overlap minimisation is done using a spot overlap matrix 'M' that includes the amount overlap between spots in a pair-wise manner i.e. matrix element M_{ij} represents the overlap between spot i and spot j. The overlap matrix is therefore defined as:

$$M_{ij} = \sum_{k}^{all\ voxels} (d_{ik} \geq T) * \left(d_{jk} \geq T\right) \tag{6}$$

where M_{ij} is the total number of voxels that overlap between spot i and j, d_{ik} and d_{jk} are the dose contributions of the spots, and T is the threshold defining the minimum required dose contribution of a spot to a voxel. The threshold T is set to 0.01 Gy since this corresponds to the threshold used for PBS delivery time. During optimisation, the overlap matrix is minimised in a quadratic way:

$$\min_{\bar{x}}(overlap) = \min_{\bar{x}}(\bar{x}^T M \bar{x}) \tag{7}$$

Where $\bar{x}$ contains all the spot weights as described in chapter 2.1. Two variations of spot overlap minimisation are implemented: Full-plan overlap and beam-wise overlap. For full plan overlap optimisation, all spot pairs are used. For beam-wise overlap optimisation, the overlap matrix M is created using only spot pairs from within the same beam. In other words, spot pairs consisting out of spots from different beam angles are not considered. The latter is of special benefit for a 1 beam per fraction approach where minimising spot overlap from different fractions is not useful.

The spot overlap minimisation is added as an objective to the wish list in the treatment planning system with a priority of 3. This means its priority is below target objectives but above healthy tissue objectives. This way, the following order is followed during treatment planning: First, the objectives considering PTV and GTV doses are optimised that determine the required spots and spot weights for target irradiation. Based on these values, the spot overlap matrix is calculated. Then, using the overlap matrix, spot overlap minimisation is performed to find a solution of target irradiation with minimum spot overlap. Hereafter, the objectives considering healthy tissue are optimised. Note that all objectives are minimised within the boundaries of the constraints on target dose and OARs. The full wish-list containing all objectives and constraints can be found in appendix A. To evaluate the influence of the described overlap optimisation on treatment plans, spot overlap distributions are generated, showing the total spot overlap within a treatment plan.

3

Results

3.1. PBS delivery time of a field

Artificial, circular fields are generated using varying numbers of spots and optimised for different target doses to vary the contribution of travel time. Additionally, the irradiated area is varied by turning off spots. For every combination, the PBS delivery time is calculated for circular and row-wise scanning. In figure 4, the delivery times are plotted as function of field size for three target doses. As illustrated, circular scanning is less efficient compared to row-wise scanning, found for both mean and maximum PBS delivery time. As the irradiated area is enlarged, the relative difference between row-wise and circular scanning increases. Starting from around 15 σ^2, the delivery time appears to be linearly dependent on field size.

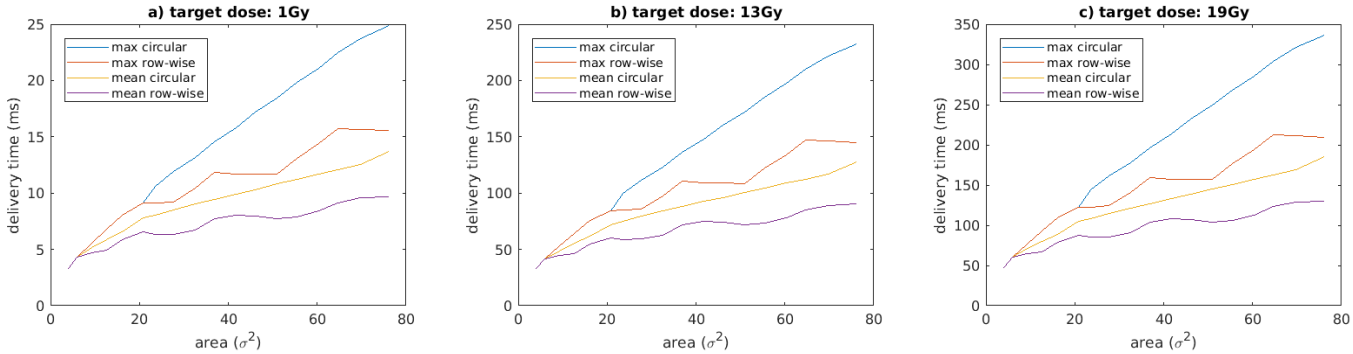

Figure 4: Pencil beam scanning (PBS) delivery time as a function of area for 1, 13 and 19 Gy fields, generated with spots 1 standard deviation (σ) separated from each other. Since the scanning pattern significantly influences delivery-time distributions, both maximum and mean values are plotted for circular vs row-wise scanning. Row-wise scanning outperforms circular scanning increasingly as the irradiated area grows looking at both maximum and mean delivery times.

The PBS delivery time within a field also depends on spot separation. In other words, given any defined circular field, irradiated with uniformly distributed spots, the delivery time for this field is dependent on the number of spots used. Illustrated in figure 5, it can be seen that an advantage is found for fields irradiated with spots at larger separation. Row-wise scanning still outperforms circular scanning on both maximum and mean delivery times for all spot separations.

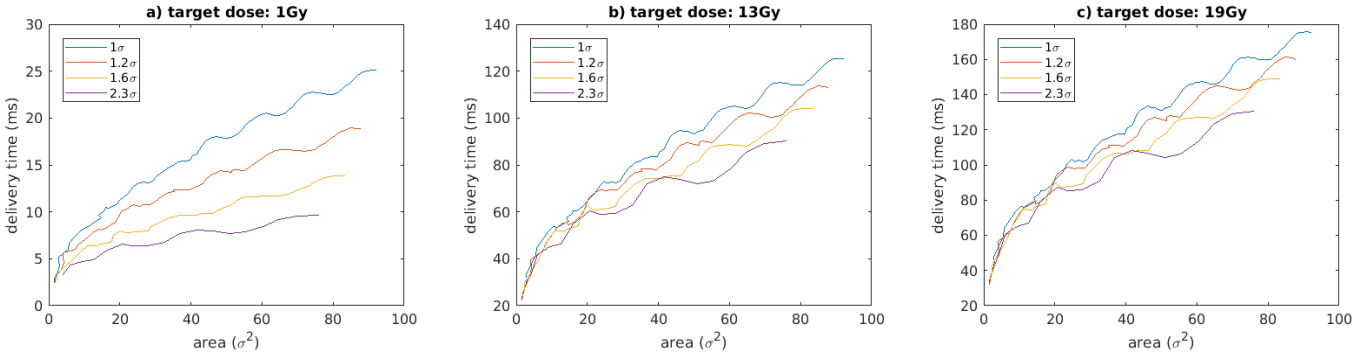

Figure 5: Mean row-wise PBS delivery time as a function of area for fields generated using uniformly distributed spots 1, 1.2, 1.6 and 2.3 standard deviations apart. Reduction in mean delivery time is found when increasing spot separation. This effect is larger for bigger field sizes.

Assuming that a standard deviation of a pencil beam is about 3 mm, no practical boundary on field size due to delivery time is observed for a target dose of 1 Gy. The largest field size deliverable with a mean PBS delivery time of 100 ms is 765 mm^2 for 13 Gy and 315 mm^2 for 19 Gy. Assuming a spherical tumour, this results in a PTV volume of 9 cc for 13 Gy and 2 cc for 19 Gy. Of course, these volumes will further increase when even more inhomogeneity is allowed.

Given that delivery time within a field reduces when spot separation is increased, steering treatment plan optimisation towards solutions that have large spot separation might therefore benefit the PBS delivery time and thus the FLASH effect within a treatment plan. One way to increase spot separation is by minimising the spot overlap. For this reason, spot overlap minimisation is implemented in the treatment planning system.

3.2. FLASH treatment plan evaluation

Per patient, different plans were created with 3,5 and 7 beams, each optimised in three versions: optimisation on dose only, dose + total plan spot overlap, and dose + beam-wise spot overlap. In total, 54 treatment plans were obtained. Overall, most difficulties were encountered during treatment planning for patient 1. Doses in the OARs were unavoidable and led to clinical constraint violation of the spinal cord for the 5 and 7-beam plans. In some treatment plans, a Bragg peak was found inside the patient. These plans are: Patient 2: 3 and 5 beams, and patient 6: 3, 5 and 7 beams.

3.2.1. Spot overlap

Spot overlap is evaluated using overlap distributions that show the number of overlapping pencil beams per voxel. Since we are only interested in decreasing the overlap within healthy tissue, values within the PTV are not shown. In all cases, both full-plan and beam-wise overlap optimisation show a great reduction in overlap values within spot-overlap distributions. The full-plan optimisation induces a larger reduction compared to beam-wise optimisation. Although the same optimisation is performed each time, the achieved amount of overlap reduction varies per patient and plan. For example, in patient 1, the maximum overlap value for the 3-beams plan was reduced from 45 to 43 overlapping spots. For the 5-beams plan, the reduction was much larger, from 65 to 43 overlapping spots. In figure 6, two examples are given for the spot overlap reduction.

Since the goal of spot overlap minimisation is to increase spot separation, the spot positions per beam are also evaluated. It is found that, in general, the overlap minimisation reduces the number of spots used for irradiation and therewith increases spot separation as visualised in figure 7.

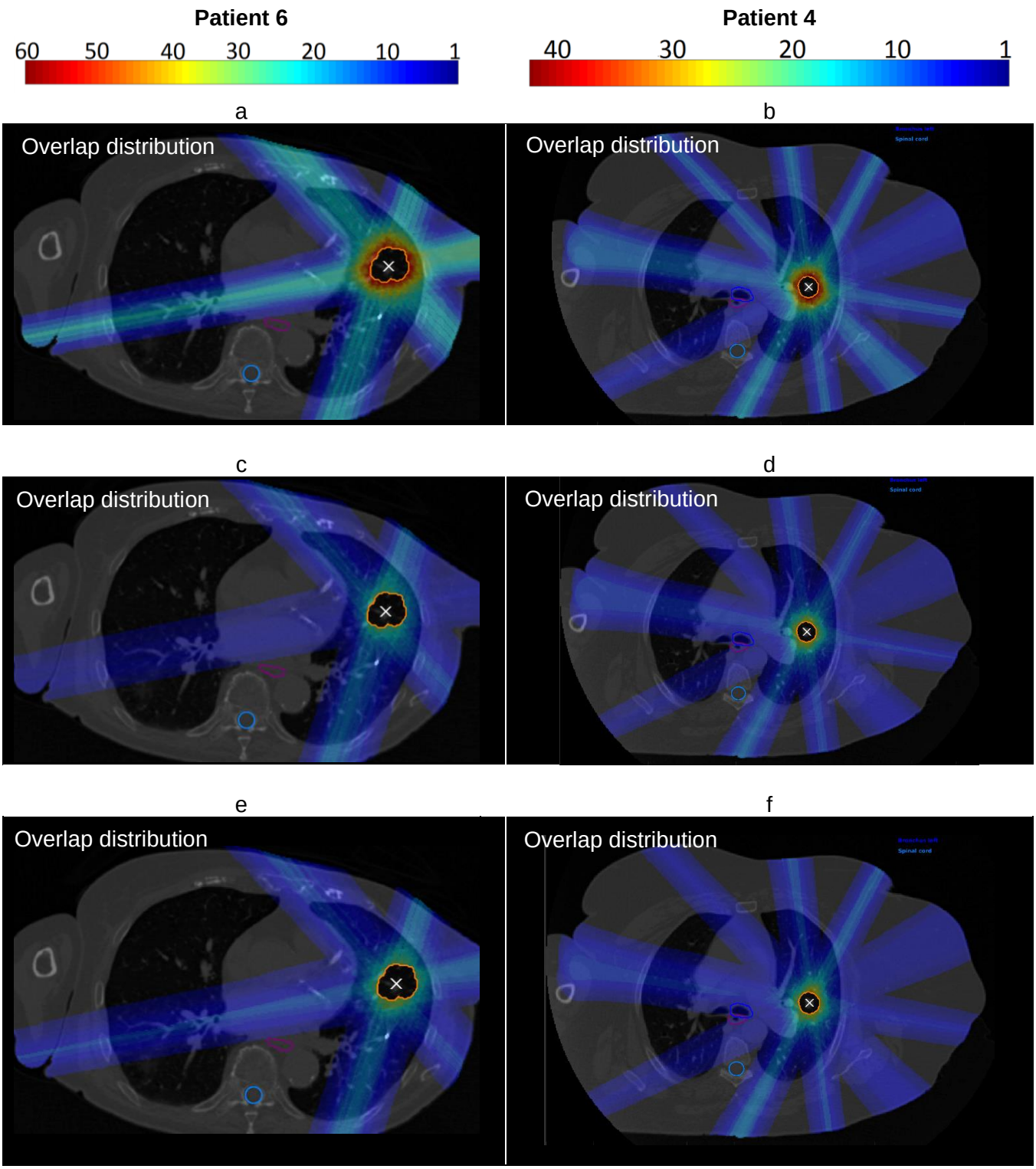

Figure 6 spot overlap distribution for a 4-beams plan of patient 4 (left) and a 5-beams plan for patient 6 (right) with no overlap optimisation (a,b), entire treatment plan spot overlap minimisation (c,d) and spot overlap minimisation within each beam (e,f). The organs at risk and target structures are delineated by orange for PTV, light blue for the spinal cord, dark blue for the bronchus and purple for the trachea. Overlap is not shown inside the PTV since overlap inside the target is not of interest. Full overlap minimisation shows a great reduction in overlap compared to no optimisation. Beam-wise optimisation shows less reduction.

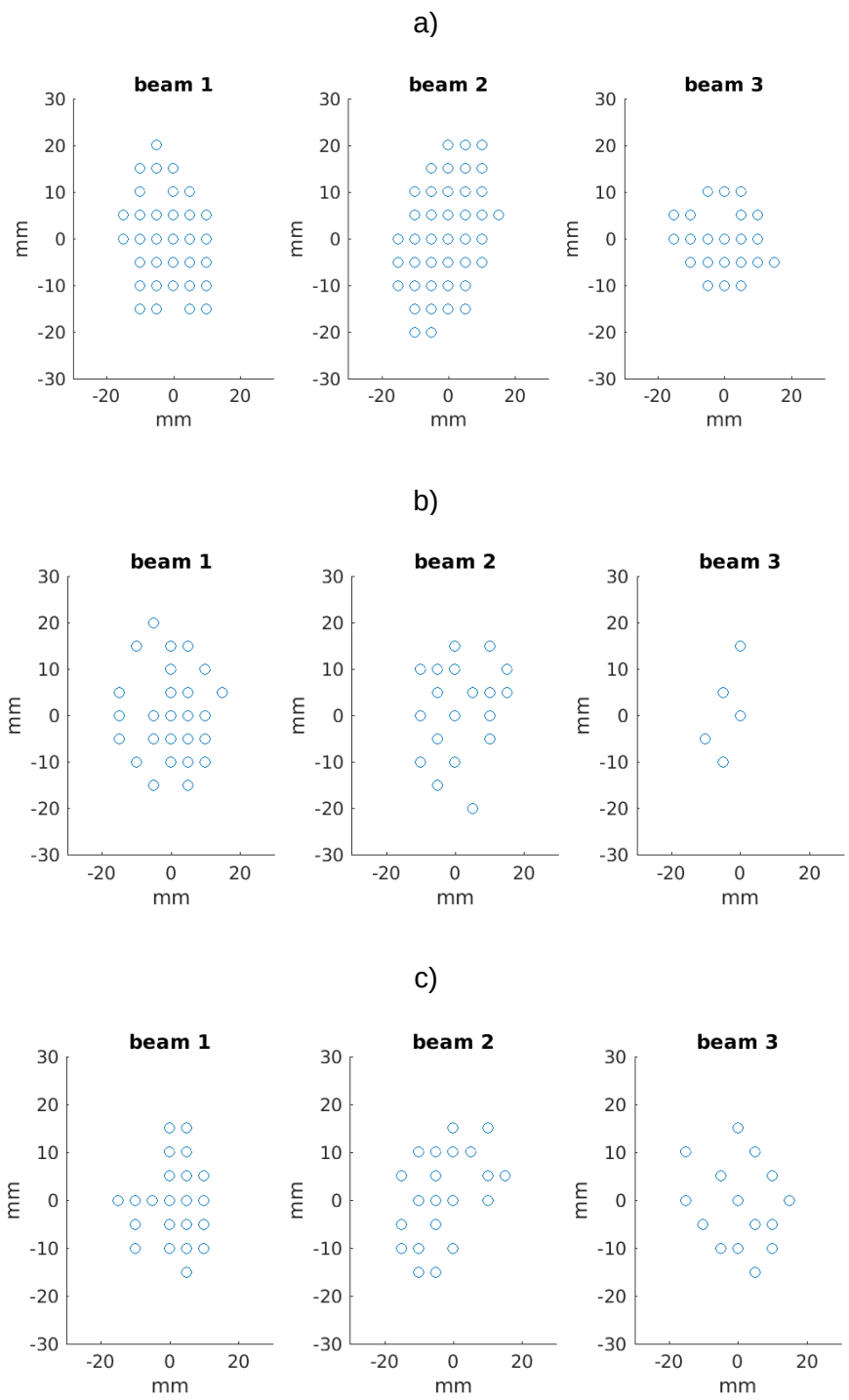

Figure 7: Spot distributions of the 3-beam plans, generated for patient 4 with no optimisation on spot overlap (a), optimisation on spot overlap within the entire plan (b) and spot overlap optimisation only within the beams (c). Full plan overlap minimisation induces the largest reduction in number of spots and increased spot separation. Beam-wise overlap minimisation shows less reduction in spot overlap and less increase in spot separation.

3.2.2. Evaluation on delivery time

As mentioned in chapter 3.2.1, spot overlap reduction successfully increases spot separation. However, although predicted in chapter 3.1, this does not guarantee reduction in PBS delivery time. To investigate the influence of spot overlap optimisation on delivery time, PBS delivery-time distributions and delivery-time-volume histograms are analysed. The PBS delivery times are found to increase for most beams per plan, while significantly decreased (improve) for one beam inside a treatment plan. Figure 8 shows how this effect can be so extreme that it diminishes the delivery times from a beam.

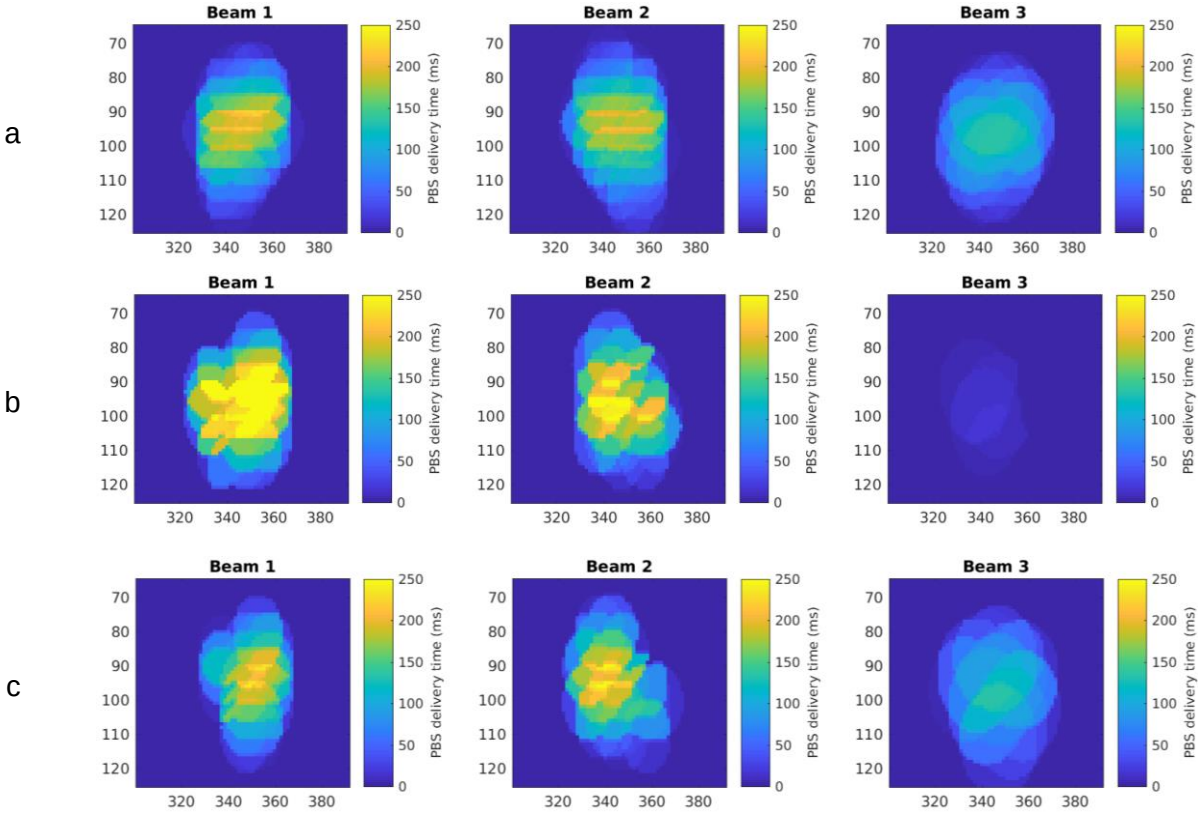

Figure 8: Beam slices showing the distribution of pencil-beam scanning (PBS) delivery times from the 3-beams plan generated for patient 4. Without optimisation (a), spot overlap minimisation on all spots in the treatment plan (b) and beam-wise minimisation on spot overlap (c). For beam 1 and 2, the PBS delivery time was increased after optimisation on spot overlap. The entire treatment plan overlap minimisation induced the largest increase in PBS delivery time for these beams. The contrary happened for beam 3, a significant reduction in PBS delivery time is found for beam-wise overlap minimisation and even more so for full plan overlap minimisation.

The effect can also be noticed when looking at the delivery-time-volume-histograms. The largest reduction is often found for only a single or few beams. For example, the delivery-time-volume histograms of the 3-beams plans of patient 4, depicted in figure 9, show a significant reduction in delivery time only for beam 3. The delivery times even increase for beam 1. These effects are also present when investigating the delivery times for all voxels that receive a dose exceeding 10 Gy, shown in figure 10. Another thing that can be observed from both the delivery-time distributions and the delivery-time-volume histograms is that PBS delivery time strongly varies within and between each beam, ranging from 0 to 350 ms. For all plans, a large portion of voxels experience delivery times below 100 ms, ranging from about 20 to 80 %. Increased number of beams per plan reduces the delivery time per beam. The 7-beams

plan of patient 6 is the closest to full FLASH irradiation times with maximum PBS delivery times in beams of 85.0, 102.5, 104.4, 93.7, 89.7, 63.6 and 94.2 ms for beam 1 to 7 respectively. The overlap, spot, PBS delivery time and dose distributions of this case can be found in appendix C.

The PBS delivery time is composed out of travel times and spot irradiation times. The contribution of travel times to the maximum PBS delivery time is mostly less than 10 percent, ranging between 2.8 and 24.8 ms. The maximum and mean delivery times, and the travel times of all treatment plans can be found in appendix B.

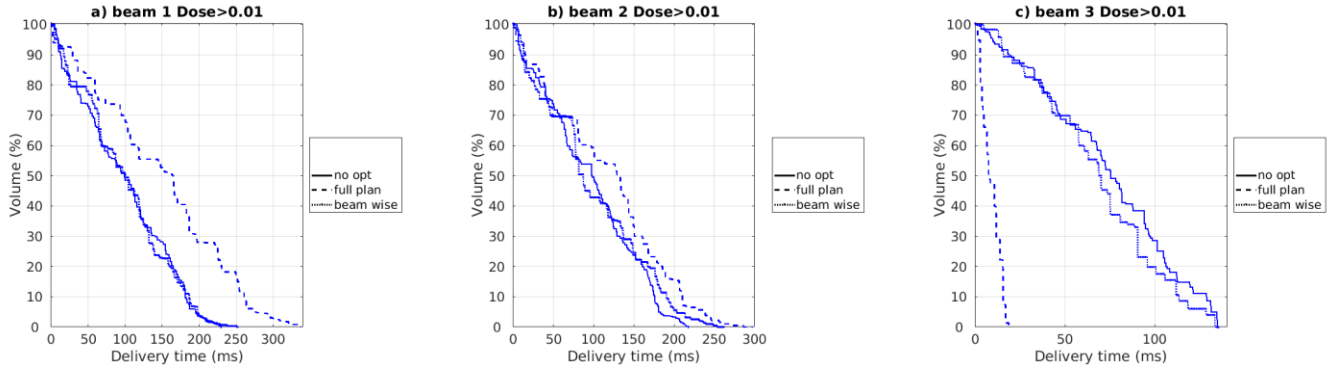

Figure 9: Delivery-time-volume histogram of the 3-beams plan created for patient 4. Full plan spot-overlap optimisation increases the delivery time of beam 1 while significantly decreasing the delivery time of beam 3. Beam-wise spot-overlap minimisation does not impact the delivery times significantly.

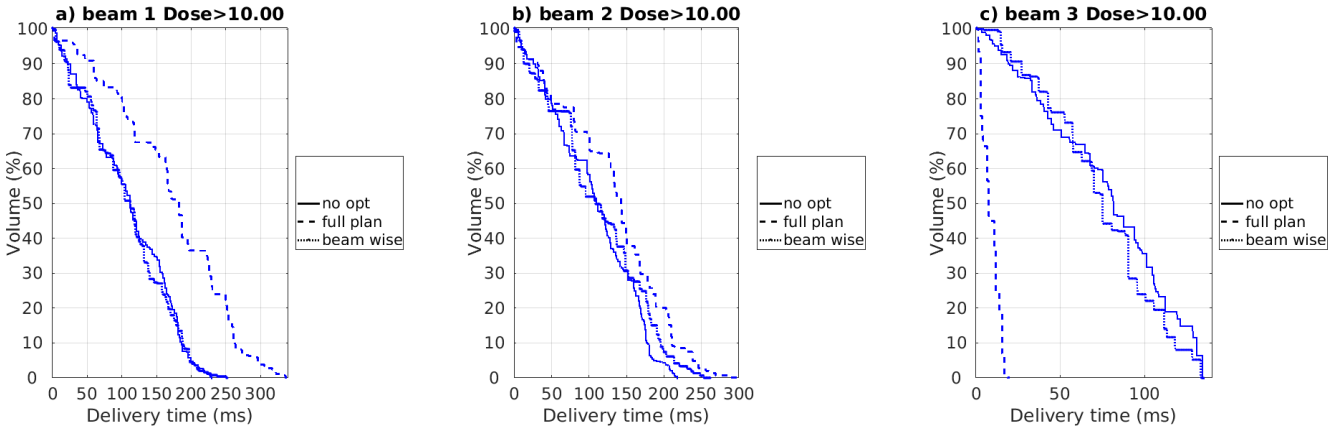

Figure 10: Delivery-time-volume histogram of the 3-beams plan created for patient 4. Only voxels that receive a dose exceeding 10 Gy are used. Full-plan spot-overlap optimisation increases the delivery time of beam 1 while significantly decreasing the delivery time of beam 3. Beam-wise spot-overlap minimisation does not impact the delivery times significantly.

3.2.3. Evaluation on dose-rate

Evaluation on dose rate is done using dose-rate-volume histograms. In general, no clear overall improvement of dose rates can be seen when optimising on spot overlap. Nevertheless, in some cases, an increase on dose rates could be observed for certain beams when using a full plan spot overlap optimisation. However, a distinct improvement as seen in the irradiation-time-volume histograms is not visible. For example, in figure 11, it can be seen that the dose rates have improved mostly for a single beam while only slight changes are visible in the other beams. However, the same behaviour cannot be concluded from all treatment plans.

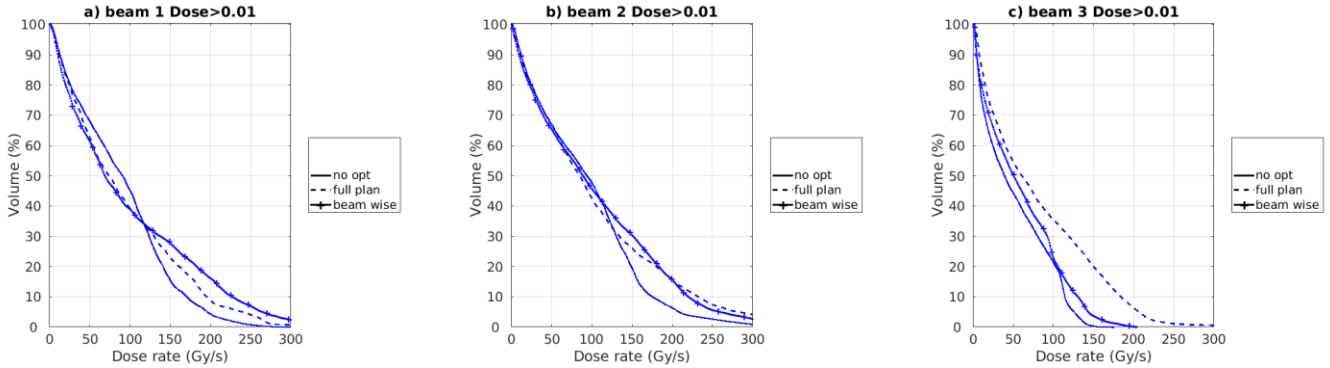

Figure 11: Dose-rate-volume histograms of the 3-beams plans created for patient 4. With respect to the treatment plan without spot overlap optimisation, full plan spot overlap minimisation increases the dose rates of the beams most for beam 3 as the entire curve is shifted to the right. For beam 2, a slight improvement can be seen. For beam 1, no overall improvement can be found. The beam-wise optimisation method only shows a small increase in dose rates for beam 2.

3.2.4. Evaluation on dose

All generated treatment plans are evaluated using dose distributions and dose-volume histograms. Not all optimisations seemed feasible, this results in violations of clinical constraints. For patient 1, the 5 and 7-beam plans violate the constraints on the spinal cord. Maximum doses in the spinal cord are 36.5 and 35.6 Gy for the 5 and 7 beam plans respectively without spot overlap optimisation, 23.5 and 22.6 Gy for full-plan optimisation, and 24.6 and 24.5 Gy for beam-wise optimisation.

All beams deliver doses mostly exceeding the FLASH target threshold of 10 Gy. In general, the high dose areas in the dose distributions of the plans optimised on spot overlap are less conform to the PTV and contain larger areas with high healthy tissue doses compared to the plans without spot overlap optimisation. The effect is larger for full plan optimisations than for beam-wise optimisations. The lack of conformity varies largely over the patients. For example, as can been seen in figure 12, for the 3-beam plans of patient 4, the high dose region highly deviates from the PTV and large high dose areas are introduced in healthy tissue. In patient 6 on the other hand, the 5-beams-plan dose distribution is surprisingly similar for optimised vs non-optimised plans.

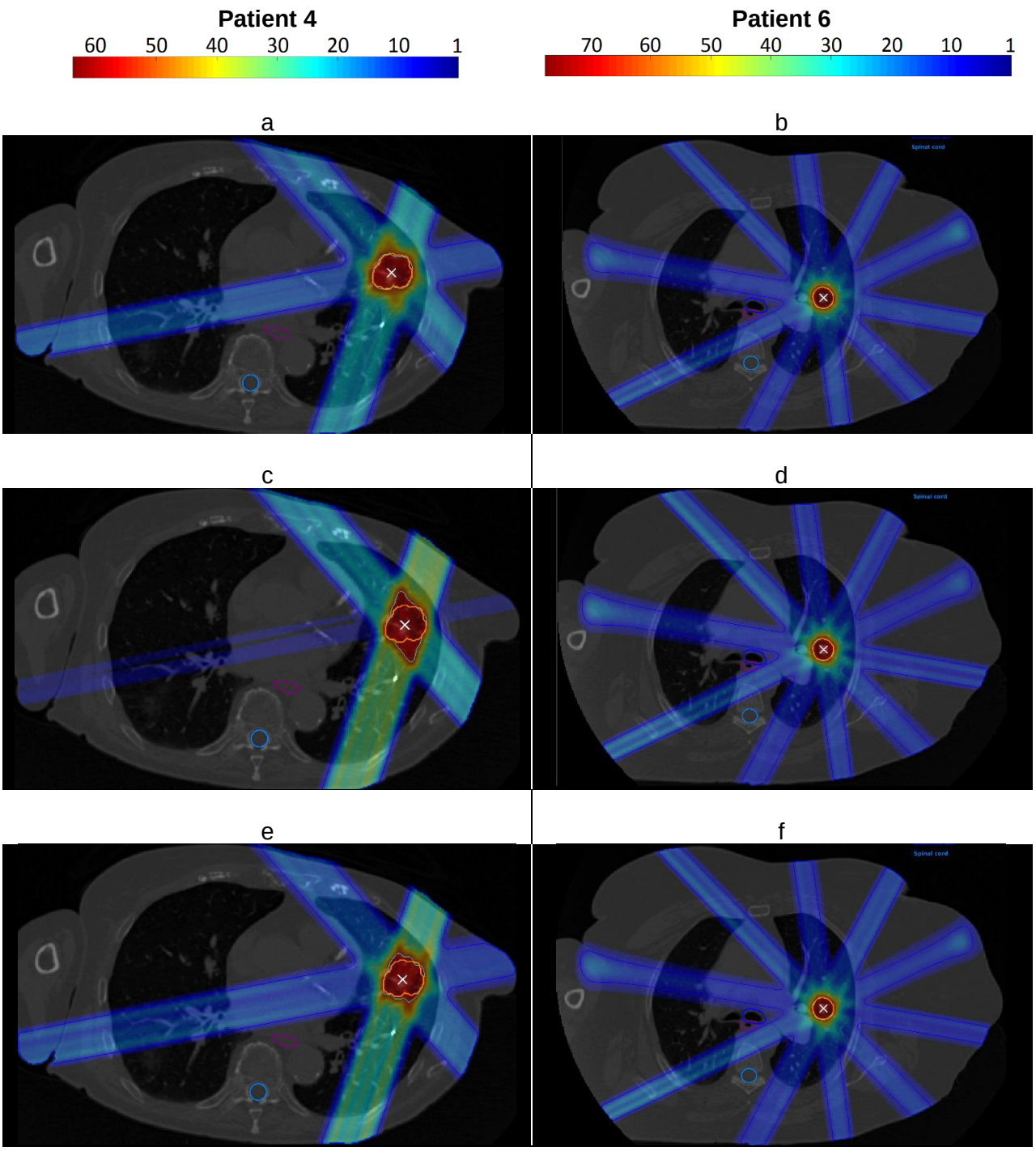

Figure 12: Dose distribution of a 3-beams plan of patient 4 (left) and 5-beams plan of patient 6 (right). The PTV is shown with an orange border line, oesophagus with purple, ipsilateral bronchus with dark blue and the spinal cord is shown in light blue. The 10 Gy isodoseline is dark blue and the isodose line equal to the target dose is (when visible) light blue. The 5-beam treatment plans of patient 6 contain Bragg peaks in healthy tissue for beam 2 and 6. Full overlap optimisation (c, d) result in a less conform solution than beam-wise optimisation (e, f) and far less conform compared to no spot overlap optimisation (a, b). The reduction of dose conformity to the PTV is significantly less for patient 6 compared to patient 4.

To further investigate the effect of spot overlap minimisation on dose, dose-volume-histograms are made for the target- and OAR structures of all treatment plans. In figure 13, example dose-volume histograms are shown that represent the overall behaviour. As can be seen in figure 13a, the dose difference between the GTV and PTV reduces as spot overlap minimisation is introduced. This means that the dose is less peaked and becomes more homogeneous within the PTV. From 13b can be observed that spot overlap minimisation does not significantly impact the dose delivered in the OARs. However, the ipsilateral lung does always contain high doses caused by the fact that the structure includes the PTV and GTV. Nevertheless, clinical V_{13} constraints are never violated.

a

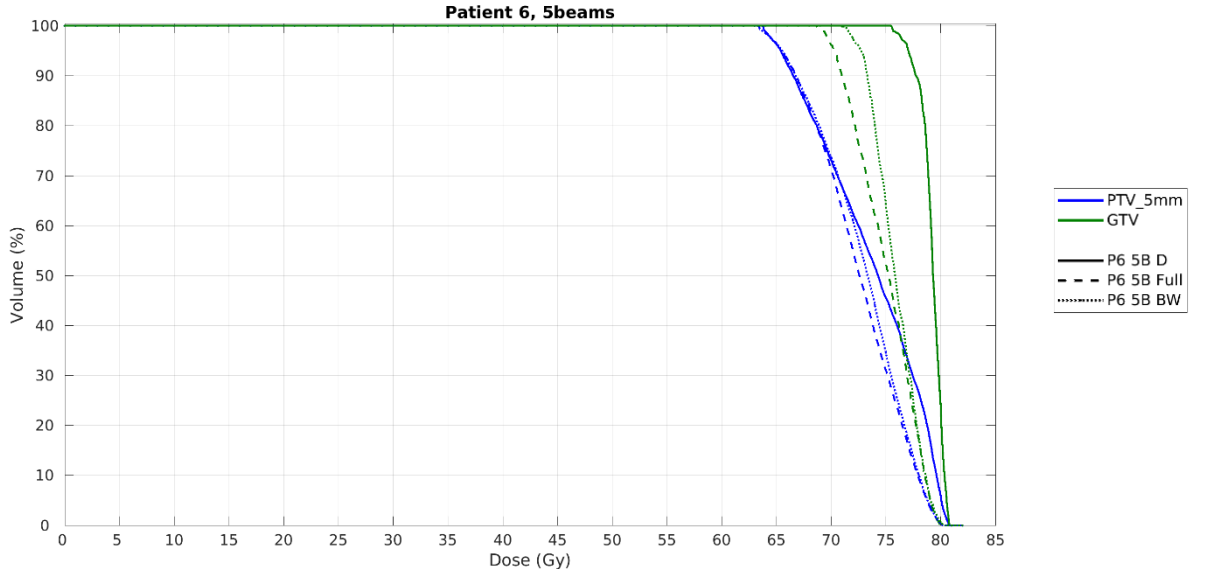

b

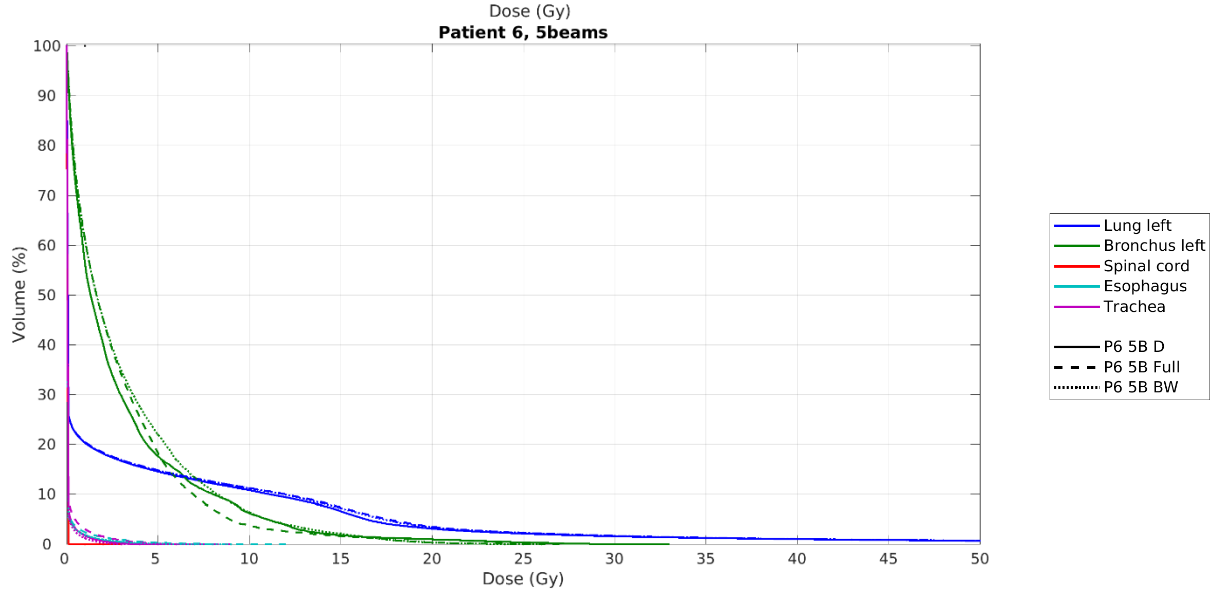

Figure 13: Dose-volume-histograms for the target structures (a) and organs at risk (b) in the 5-beams plan of patient 6. No optimisation (straight line), full treatment plan spot overlap optimisation (dashed line) and beam-wise spot-overlap optimisation (small dashed line). For the organs at risk (OARs), no significant difference is found when comparing the different optimisations. For target structures, the dose difference between the PTV and GTV is reduced when optimising on spot overlap.

4

Discussion

4.1. FLASH field irradiation

The PBS delivery time for a circular, homogeneous field depends on the spot separation and therewith the number of spots used to irradiate the field. The PBS delivery time is dependent on the number of Giga-protons delivered and total travel time. It is therefore expected that, when irradiating any field using less spots, less travel time will be involved that result in lower PBS delivery times. Furthermore, it is expected that with larger spot separation, less spot overlap will occur and thus reduces the PBS delivery time. However, given that spots need to overcompensate to deliver sufficient dose to areas in-between spots, more monitor units are delivered per spot for larger separation. This increases delivery time. Nevertheless, the latter seems to be inferior to the shortening caused by fewer spots at larger separation since delivery time decreases as spot separation increases and more heterogeneity in field dose is allowed. These results are found for our modelled, circular fields, with uniformly distributed spots but do not seem to generalise to fields for clinical practice. This could be due to the fact that tumours are not perfectly spherical, resulting in non-circular fields. Furthermore, due to treatment plan optimisation using multiple fields (beam angles) and clinical constraints such as dose limits for organs, spots are often not uniformly distributed, and spot weights strongly vary within fields. Therefore, the impact of spot separation on delivery time might be different in clinical treatment plans. Furthermore, in practice, spot separation can only be extended up until the maximum allowed dose heterogeneity is achieved.

PBS delivery times are calculated for row-wise pencil-beam scanning and circular pencil-beam scanning. The PBS delivery time distribution and corresponding values are found to highly depend on the scanning pattern. For example, row-wise scanning results in a characteristic horizontal disk-like shape as can be seen in the visualisations of figure 8. For circular scanning, the delivery time distribution shows a ring. Because of the large variations in delivery-time distribution and values, optimising the scanning pattern can improve the PBS delivery time. Here, optimisation can be done with different goals such as decreasing maximum or mean delivery time or maximising the volume that receives delivery times within the FLASH irradiation time constraint. Another phenomenon occurring for row-wise scanning is the wave-like signal on top of the lines in figures 4 and 5. Since this does not occur for circular scanning, these waves probably originate from the circular shape of the field in combination with the scanning pattern and the way the field size is varied. Since for row-wise scanning, the horizontal extend is most dominant for the delivery time, spots can be added that do not impact the delivery time but do increase the field size. For example, when adding spots to the top and bottom of the field, the maximum delivery time will not increase while the irradiated area is. However, adding spots to the left and right sides of the field impacts maximum delivery time. Furthermore, the increase in mean delivery time is also dependent on the location of added spots. Adding spots on the top or bottom only impacts the delivery time of a limited number of voxels whereas adding spots to the left and right will alter the irradiation interval time of a

larger portion of voxels. This would explain why the wave-like behaviour is found for both mean and maximum delivery times for row-wise scanning but not for circular scanning.

4.2. Spot overlap optimisation

The spot overlap optimisation successfully reduces the spot overlap within a treatment plan. Additionally, the optimisation increases spot separation and reduces the number of spots used. However, although reduction in spot overlap was always found, increase in spot separation is not present in all plans. This could be explained by the fact that the loss function used for overlap minimisation (equation 7) includes spot intensity. The optimisation therewith prioritises overlap from spots with higher spot weights. Of course, one way to reduce the overlap is by deleting spots. However, there also might be optima for the loss function where spots are reduced but not completely removed, thus showing no change in number of spots or spot separation.

There are a few aspects on which the optimisation can still be improved: First of all, the overlap matrix is only calculated before starting overlap optimisation and remains constant during optimisation. However, the dose threshold is currently set at 1cGy. Voxels that are optimised to be below the threshold are still counted as overlap during optimisation. Likewise, the optimiser could increase the dose in voxels that were below the threshold when generating the overlap matrix and therewith increase the overlap while decreasing the cost function. Although the impact of this behaviour of the optimisation is currently unknown and might be insignificant, it could change if the dose threshold is varied. Secondly, the lateral grid spacing, on which spots are positioned is currently set to 5mm. Decreasing the lateral spacing of the grid on which spots are positioned lead to more possible locations of spots and could therefore increase the freedom for spot overlap optimisation. Finally, the spot overlap matrix ‘M’ only considers pair wise overlap. It does therefore not differentiate in number of contributing spots. For example, voxels that receive dose from only 2 spots are treated equally as voxels that receive dose from 20 spots. Including prioritisation on the number of contributing spots can create more targeted optimisation. E.g., more focus could be placed on optimising the areas with high amount of spot overlap, that are likely to be in the centre of the beams. Increasing spot separation here might have a larger impact on maximum PBS delivery time compared to spots on the outer side of the beam. Likewise, one could argue for the opposite, focus overlap reduction in areas that are more sensitive to reduce the number of contributing spots and therewith have a larger impact on total overlap. Implementing an overlap optimisation that includes some kind of prioritisation could therefore result in more preferable behaviour.

Full-plan overlap optimisation has a larger impact than beam-wise optimisation on all evaluations i.e. spot overlap distribution, spot separation, number of spots, PBS delivery time and dose rate. This is expected for spot overlap distribution. However, it is not trivial that full-plan optimisation reduces the number of spots more or increases spot separation within beams to a greater extend. This is unexpected since beam-wise optimisation solely targets spot overlap of beam pairs within the same beam angle and is therefore more specialised in increasing spot separation and therewith reducing the number of spots within beams. However, as discussed earlier, minimising the loss function does not directly decrease the number of spots nor directly increases spot separation. Furthermore, since beam-wise optimisation is non-convex, it could be possible that a local minimum was found rather than a global minimum.

4.3. FLASH treatment plan evaluation

Creating proton transmission beam treatment plans using 3, 5 and 7 beams was possible for all patients. Unfortunately, some treatment plans contain a Bragg peak in the patient. This leads to high doses inside healthy tissue and is unwanted. However, in most of the cases, the Bragg peak occurs in the patients' arm. An arm support would be sufficient to prevent it from happening. Furthermore, the energy used in the current treatment plans is 244 MeV. In practice, the cyclotron can deliver 250 MeV, shifting the Bragg peak slightly further, potentially out of the patient. Nevertheless, in practice, the possible beam angles might be limited for very large patients. This will lead to reduced treatment plan quality and might make transmission beam irradiation unsuitable for some patients.

The results of this study are in-line with that of earlier studies done on FLASH IMPT treatment planning. For example, van de Water *et al*. also concluded that reducing the number of spots, hypofractionation and transmission beams are necessary to achieve FLASH-compatible dose rates [25]. However, van de Water *et al*. put most emphasis on dose rates while this study investigates irradiation time and dose too as important FLASH factors. Taking the whole FLASH triangle into account is more in agreement with the conclusions drawn by van Marlen *et al*. : "It currently seems logical to optimise plans for the shortest delivery time, maximum amount of high dose rate coverage, and maximum amount of single beam and continuous irradiation." [24]. However, van Marlen *et al* does not take the importance of a minimum required dose into account as is done in this study. Further discussion on the evaluation criteria used by van de Water *et al*. and van Marlen *et al*. can be found in the literature study in appendix D.

4.3.1. Evaluation on dose

Dose distribution of the treatment plans highly differ per patient. Both tumour size and position play an important role in dose conformity to the PTV and OARs avoidance. With larger number of beams, completely avoiding OARs becomes harder, sometimes negatively affecting the treatment plan quality. Furthermore, some beam angles seem to be less suitable for dose delivery. These beams cover longer distance within the patient and sometimes even contain a Bragg peak inside the patient. Beam angle optimisation can provide a solution for both cases. When inspecting the influence of spot overlap minimisation on the dose distribution, it seems that the optimisations tend to shift the relative dose contributions from the beams to decrease spot overlap. The dose contribution is reduced of beams with less suitable beam angles, i.e. beams that cover a large distance in the patient. This reduction is then compensated for using the other beams. This behaviour decreases the overall spot overlap but often impacts the high dose area conformity. In some cases, the high dose areas get so large that the treatment plan will most probably not be clinically acceptable. The effect is less abundant for beam-wise optimisation. The sacrifice of dose distribution to delivery time and dose rates found in this study is expected given the FLASH triangle. Optionally, the wish-list priorities could be altered such that dose conformity gets more importance. However, the freedom for optimisation on spot overlap will be less and the effect of it will therefore be less too.

4.3.2. Irradiation time

The delivery times vary largely both between beams and within beams. Contrary to the effect on dose, spot overlap optimisation improves the delivery times for beams that are less suitable for dose delivery. However, this improvement is at the expense of the other beams. This is expected since the delivery time is dependent on the number of Giga-protons delivered and therewith dependent on dose. Nevertheless, the DTVHs visualised for voxels that receive a dose exceeding 10 Gy still show a similar improvement in delivery time. Therefore, the dose is still high enough to expect a FLASH effect. The FLASH potential is thus improved by spot overlap optimisation for certain beams.

As found in the results of circular field irradiation modelling in chapter 3.1., delivery time is dependent on field size. This characteristic can also be found for the patient study. Linking the maximum and mean PBS delivery times (appendix B) with the corresponding PTV volumes (table 2), it is found that PBS delivery times increases with PTV size. The delivery times decrease when more beam angles are used since this requires lower doses per beam. Therefore, because of the small PTV size and large amount of beam angles, the 7-beam plans for patient 6 can be delivered within FLASH delivery times. Although other plans are further away from the FLASH irradiation time threshold, in all plans, large volumes experience a PBS delivery time lower than the targeted 100 ms. This means that large volumes of healthy tissue will probably experience a FLASH effect, improving the patient's treatment. This improvement might be even larger in practice considering that the 100 ms threshold used in this study is somewhat conservative. It is still unknown if there is a threshold and if it exists, what value should be given to it. Studies have found a FLASH effect for irradiation times exceeding 100 ms, up to 500 ms [3], [4], [6]-[10], [20], [27]. If the threshold turns out to be higher than our current value, more, if not all treatment plans generated in this study could be considered full FLASH plans. Nevertheless, given the large uncertainties around the FLASH effect, it is important to take a conservative approach. Therefore, delivery times should be aimed to be as low as possible.

Whether or not a treatment plan can be delivered within a given irradiation time is also dependent on the definition of irradiation time. The PBS delivery time, used in this study, is a good way to describe the delivery time as experienced per voxel. When using pencil-beam scanning, not all tissue is irradiated at once. Therefore, this definition might be closer to the true irradiation time as experienced by the tissue than total beam irradiation times. However, this approach makes use of some assumptions. First of all, defining the presence of a FLASH effect based on PBS delivery time assumes that the FLASH effect is purely a local effect. Although this would be in-line with certain theories e.g. radiolytic oxygen depletion, it could be possible that global effects play a role in the mechanics of FLASH such as circulating immune cell sparing. In those cases, the entire beam irradiation time would be more appropriate. Secondly, the results of PBS delivery time are dependent on the 1cGy threshold. This threshold is arbitrary chosen and effects the values of the delivery times. Different dose thresholds will result in different delivery times and therewith varying predictions about the FLASH abundance within a treatment plan.

The use of pencil-beam scanning itself for FLASH irradiation is also questionable. No study thus far has investigated the FLASH effect using pencil-beam scanning nor investigated the effects of similar tissue revisits. It is therefore not certain if a FLASH effect can be expected at all when a patient is treated this way. Nevertheless, if FLASH irradiation using PBS turns out to be possible and FLASH appears to be a mainly local effect, intensity modulation using PBS will have an advantage over passive scattering methods. This is because when passive scattering is used, the complete field is irradiated at once. This makes the delivery time constant over the entire field and defined by the maximum dose. Due to the very local dose delivery of spots in PBS, the PBS delivery time varies throughout the field and will therefore be lower in most areas.

The PBS delivery time could be even further cut down by reducing the travel times between spots. Since intermediate position confirmation consumes most of the travel time, it could be possible to improve travel times and therewith irradiation times by adopting a different quality assurance approach. Nevertheless, the travel times turn out to only consume a small fraction <10% of the delivery time. In most cases, this will not be enough to shift a treatment plan into FLASH domain. Finally, another improvement on delivery time could be gained by optimisation of the scanning pattern as discussed earlier.

4.3.3. Dose rate

Similar to the irradiation time, dose rates seem to improve for less suitable beams after spot overlap minimisation. However, the improvement in dose rate, shown in figure 11c, is less abundant than the improvement of irradiation time seen in figure 9c and 10c. This leads us to think that some of the improvement on irradiation time was done in low-dose areas. Nevertheless, an improvement in dose rate was still found when only inspecting doses exceeding 10 Gy. If all doses are above the FLASH threshold of 10 Gy and irradiation times below its threshold of 100 ms, given equation 1, it automatically follows that the dose rates are sufficiently high. Evaluation on both dose and irradiation time is therefore enough to fully evaluate the FLASH potential within a treatment plan. Nonetheless, investigating the dose rates is important since previous FLASH studies often solely report dose rates rather than delivery-time-dose combinations. To maintain comparison between studies, all irradiation and delivery parameters should be reported.

5 Conclusions

The PBS delivery times within a field seem to depend on (i) target volume and (ii) the delivered dose. The most PBS-delivery-time efficient way to irradiate a field is by using as little spots as possible, or in other words, enlarge spot separation as much as possible.

Based on this finding, spot overlap minimisation was implemented in the treatment planning system to increase the spot separation within fields as to reduce the PBS delivery times and thereby increase the FLASH potential within a treatment plan. Two versions of spot overlap optimisation were implemented, (i) full plan optimisation, spot overlap minimisation between all spots within the entire treatment plan and (ii) beam-wise optimisation, spot overlap minimisation only between spots delivered using the same beam angle. To test the FLASH optimisation method, treatment plans were generated with and without FLASH optimisation for 6 small lung tumour patients with varying PTV sizes. To ensure adequate dose, the treatment plans were created using only 3, 5 and 7 transmission beams.

We found that our current implementation of spot overlap minimisation does significantly reduce spot overlap within a treatment plan. Additionally, the number of spots is often decreased, and spot separation increased. However, spot overlap optimisation does not decrease the overall PBS delivery times nor does it decrease the mean dose rates within a treatment plan. Nevertheless, overlap optimisation does reduce the dose contribution of less suitable beams, i.e. beams that cover a large distance through the patient and thereby deliver relatively more dose to healthy tissue. As result, the PBS delivery times, and dose rates are improved for these beams. At the same time, the reduction of dose is compensated by the other beams. This leads to higher delivery times and lower dose rates in these beams, and the high dose areas within the dose distribution become less conform to the PTV, decreasing the treatment plan quality. Furthermore, the magnitude of the effect strongly differs per treatment plan. Spot overlap minimisation is therefore not suitable for FLASH optimisation in clinical IMPT treatment planning.

6

Outlook

In this study, we approached FLASH-RT treatment planning by using 3, 5 or 7 transmission beams, given one beam per fraction. The disadvantages of transmission beams are clearly visible: there is more irradiated healthy tissue, sparing of organs at risk is harder and there are limited treatment angles due to healthy tissue Bragg peaks. Nevertheless, it was possible to create transmission beam plans for all patients within clinical constraints. Furthermore, the benefits of proton transmission beams over photon SBRT remain. Additionally, there might even be a special benefit of transmission beams over conventional proton irradiation for certain patients with very small lung tumours since the lateral penumbra of transmission beams are relatively sharp compared to the large amount of scattering around a Bragg peak.

The one beam per fraction approach ensures FLASH compatible doses per fraction (>10Gy) and avoids tissue revisits due to beam overlap. Hypofractionation i.e. giving large doses per fraction, is not uncommon for lung tumour treatment. Nevertheless, for conventional treatment plan hypofractionation, all dose, including multiple beams, is split into multiple fractions. For the one beam per fraction approach, only the areas containing beam overlap experience some form of fractionation. This means that most of the healthy tissue will not experience a fractionation effect. Due to the lack of this, the single beam per fraction approach delivers more healthy tissue damage than the all beams per fraction delivery. The additional healthy tissue sparing gained by FLASH can overcome this disadvantage. However, this is dependent on the currently unknown dose-modifying factor of FLASH. Aside from single beam per fraction or all beams per fraction, hybrid solutions could exist where only part of the beams (fractions) are delivered using FLASH. This can be a mix of Bragg peak and transmission beams or a full transmission beam plan of which only part of the plan is given as FLASH. As stated before, within a transmission beam treatment plan, certain beams are more suitable for FLASH irradiation than others. In some cases, this difference is enhanced by overlap minimisation. Therefore, in a hybrid solution, beams suitable for FLASH can be used as FLASH boost to a conventional treatment plan. As an alternative, beam shapes can be created that only partly irradiate the tumour but satisfy the FLASH constraints. Multiple beams can still fully cover the tumour using patch working. However, due to uncertainties of radiotherapy, additional treatment margins will need to be applied to ensure full tumour coverage. This will likely counteract the patch working principle.

Spot overlap minimisation is, in its current form, is unsuitable for FLASH optimisation in clinical IMPT treatment planning. Other optimisation strategies should be investigated to improve the FLASH potential within a treatment plan. Recommended topics are optimisation on PBS delivery time or PBS pattern optimisation. Furthermore, beam-angle optimisation should be introduced in transmission beam treatment planning. Aside from this, in this study we assume an upgraded cyclotron for calculation of delivery time that has beam current of 400nA at the snout with an energy of 244 MeV. Although this is

already at the limit of the cyclotron's capabilities, further improvement on beam current will benefit the FLASH-RT overall. For example, higher beam current will result in even lower delivery times and higher dose rates. Enabling high beam current for lower energies will allow the use of FLASH Bragg peaks, improving the dose distributions and enabling FLASH-RT for other patients.

For now, FLASH IMPT will not benefit all patients. Because of the link between PTV size and delivery time, not even all patients evaluated in this study are eligible for FLASH-RT due to their tumour size. However, as discussed earlier, this is based on uncertain parameters such as the dose and delivery time thresholds, and the PBS delivery times could still be improved in various ways. Nevertheless, our implementation of FLASH treatment planning, using FLASH IMPT transmission beam plans, can only be established to be within FLASH constraints for lung patients with very small tumours, preferably located away from the OARs. At the same time, the patients cannot be too large to avoid Bragg peaks inside healthy tissue. To ensure satisfaction to FLASH constraints, the treatment plans will need 7 beams, given as single beam per fraction, delivering > 10 Gy each time.

Aside from the potential healthy tissue sparing of the FLASH effect, FLASH irradiation can have other potential benefits. The short fraction times allow for higher patient throughput, allowing proton treatment to be cheaper and available for more patients. Aside from this, since patient movement fixation can be uncomfortable, the very-short irradiation times can significantly decrease the duration of the unpleasant situation. For lung patients, the short irradiation times can improve the ability for gating and breath-holding.

7

References

[1] ‘The Erasmus MC Cancer Institute’. https://www.erasmusmc.nl/en/patient-care/about-erasmus-mc (accessed Jan. 27, 2020).

[2] ‘PTCOG - Facilities in Operation’. https://www.ptcog.ch/index.php/facilities-in-operation (accessed Jun. 16, 2020).

[3] E. S. Diffenderfer *et al.*, ‘Design, Implementation, and in Vivo Validation of a Novel Proton FLASH Radiation Therapy System’, *International Journal of Radiation Oncology*Biology*Physics*, vol. 106, no. 2, pp. 440–448, Feb. 2020, doi: 10.1016/j.ijrobp.2019.10.049.

[4] K. Levy *et al.*, ‘FLASH irradiation enhances the therapeutic index of abdominal radiotherapy in mice’, Cancer Biology, preprint, Dec. 2019. doi: 10.1101/2019.12.12.873414.

[5] P. Montay-Gruel *et al.*, ‘Irradiation in a flash: Unique sparing of memory in mice after whole brain irradiation with dose rates above 100 Gy/s’, *Radiotherapy and Oncology*, vol. 124, no. 3, pp. 365–369, Sep. 2017, doi: 10.1016/j.radonc.2017.05.003.

[6] P. Montay-Gruel *et al.*, ‘Long-term neurocognitive benefits of FLASH radiotherapy driven by reduced reactive oxygen species’, *Proc Natl Acad Sci USA*, vol. 116, no. 22, pp. 10943–10951, May 2019, doi: 10.1073/pnas.1901777116.

[7] D. A. Simmons *et al.*, ‘Reduced cognitive deficits after FLASH irradiation of whole mouse brain are associated with less hippocampal dendritic spine loss and neuroinflammation’, *Radiotherapy and Oncology*, vol. 139, pp. 4–10, Oct. 2019, doi: 10.1016/j.radonc.2019.06.006.

[8] M.-C. Vozenin *et al.*, ‘The Advantage of FLASH Radiotherapy Confirmed in Mini-pig and Cat-cancer Patients’, *Clin Cancer Res*, vol. 25, no. 1, pp. 35–42, Jan. 2019, doi: 10.1158/1078-0432.CCR-17-3375.

[9] C. Fouillade *et al.*, ‘FLASH Irradiation Spares Lung Progenitor Cells and Limits the Incidence of Radio-induced Senescence’, *Clin Cancer Res*, pp. 1078-0432.CCR-19–1440, Dec. 2019, doi: 10.1158/1078-0432.CCR-19-1440.

[10] M. Buonanno, V. Grilj, and D. J. Brenner, ‘Biological effects in normal cells exposed to FLASH dose rate protons’, *Radiotherapy and Oncology*, vol. 139, pp. 51–55, Oct. 2019, doi: 10.1016/j.radonc.2019.02.009.

[11] J. Bourhis *et al.*, ‘Treatment of a first patient with FLASH-radiotherapy’, *Radiotherapy and Oncology*, vol. 139, pp. 18–22, Oct. 2019, doi: 10.1016/j.radonc.2019.06.019.

[12] S. B. Field and D. K. Bewley, ‘Effects of Dose-rate on the Radiation Response of Rat Skin’, *International Journal of Radiation Biology and Related Studies in Physics, Chemistry and Medicine*, vol. 26, no. 3, pp. 259–267, Jan. 1974, doi: 10.1080/09553007414551221.

[13] S. Hornsey and D. K. Bewley, ‘Hypoxia in Mouse Intestine Induced by Electron Irradiation at High Dose-rates’, *International Journal of Radiation Biology and Related Studies in Physics, Chemistry and Medicine*, vol. 19, no. 5, pp. 479–483, Jan. 1971, doi: 10.1080/09553007114550611.

[14] J. H. Hendry, J. V. Moore, B. W. Hodgson, and J. P. Keene, 'The Constant Low Oxygen Concentration in All the Target Cells for Mouse Tail Radionecrosis', *Radiation Research*, vol. 92, no. 1, p. 172, Oct. 1982, doi: 10.2307/3575852.
[15] R. J. Berry and J. B. H. Stedeford, 'Reproductive survival of mammalian cells after irradiation at ultra-high dose-rates: further observations and their importance for radiotherapy', *BJR*, vol. 45, no. 531, pp. 171–177, Mar. 1972, doi: 10.1259/0007-1285-45-531-171.
[16] R. J. Berry, 'EFFECTS OF RADIATION DOSE-RATE: From Protracted, Continuous Irradiation to Ultra-High Dose-Rates from Pulsed Accelerators', *British Medical Bulletin*, vol. 29, no. 1, pp. 44–47, Jan. 1973, doi: 10.1093/oxfordjournals.bmb.a070955.
[17] T. Prempree, A. Michelsen, and T. Merz, 'The repair time of chromosome breaks induced by pulsed x-rays on ultra-high dose-rate', *Int. J. Radiat. Biol. Relat. Stud. Phys. Chem. Med.*, vol. 15, no. 6, pp. 571–574, 1969, doi: 10.1080/09553006914550871.
[18] H. Weiss, E. R. Epp, J. M. Heslin, C. C. Ling, and A. Santomasso, 'Oxygen Depletion in Cells Irradiated at Ultra-high Dose-rates and at Conventional Dose-rates', *International Journal of Radiation Biology and Related Studies in Physics, Chemistry and Medicine*, vol. 26, no. 1, pp. 17–29, Jan. 1974, doi: 10.1080/09553007414550901.
[19] J. Groen, 'How to optimise FLASH in clinical IMPT treatment planning', 2020.
[20] V. Favaudon *et al.*, 'Ultrahigh dose-rate FLASH irradiation increases the differential response between normal and tumor tissue in mice', *Sci. Transl. Med.*, vol. 6, no. 245, pp. 245ra93-245ra93, Jul. 2014, doi: 10.1126/scitranslmed.3008973.
[21] G. Adrian, E. Konradsson, M. Lempart, S. Bäck, C. Ceberg, and K. Petersson, 'The FLASH effect depends on oxygen concentration', *BJR*, vol. 93, no. 1106, p. 20190702, Feb. 2020, doi: 10.1259/bjr.20190702.
[22] E. Beyreuther *et al.*, 'Feasibility of proton FLASH effect tested by zebrafish embryo irradiation', *Radiotherapy and Oncology*, vol. 139, pp. 46–50, Oct. 2019, doi: 10.1016/j.radonc.2019.06.024.
[23] B. Mou, C. J. Beltran, S. S. Park, K. R. Olivier, and K. M. Furutani, 'Feasibility of Proton Transmission-Beam Stereotactic Ablative Radiotherapy versus Photon Stereotactic Ablative Radiotherapy for Lung Tumors: A Dosimetric and Feasibility Study', *PLoS One*, vol. 9, no. 6, Jun. 2014, doi: 10.1371/journal.pone.0098621.
[24] P. van Marlen, M. Dahele, M. Folkerts, E. Abel, B. J. Slotman, and W. F. A. R. Verbakel, 'Bringing FLASH to the Clinic: Treatment Planning Considerations for Ultrahigh Dose-Rate Proton Beams', *International Journal of Radiation Oncology*Biology*Physics*, p. S0360301619340386, Nov. 2019, doi: 10.1016/j.ijrobp.2019.11.011.
[25] S. van de Water, S. Safai, J. M. Schippers, D. C. Weber, and A. J. Lomax, 'Towards FLASH proton therapy: the impact of treatment planning and machine characteristics on achievable dose rates', *Acta Oncol*, vol. 58, no. 10, pp. 1463–1469, Oct. 2019, doi: 10.1080/0284186X.2019.1627416.
[26] S. Breedveld, P. R. M. Storchi, P. W. J. Voet, and B. J. M. Heijmen, 'iCycle: Integrated, multicriterial beam angle, and profile optimization for generation of coplanar and noncoplanar IMRT plans: iCycle: multicriteria beam angle optimization', *Med. Phys.*, vol. 39, no. 2, pp. 951–963, Jan. 2012, doi: 10.1118/1.3676689.
[27] P. Montay-Gruel *et al.*, 'X-rays can trigger the FLASH effect: Ultra-high dose-rate synchrotron light source prevents normal brain injury after whole brain irradiation in mice', *Radiotherapy and Oncology*, vol. 129, no. 3, pp. 582–588, Dec. 2018, doi: 10.1016/j.radonc.2018.08.016.

8

Appendices

Appendix A: Treatment plan optimisation wish list

Table A1: Treatment planning wish list. Objective "Spot overlap ROI" is only enabled for spot overlap minimisation. A is set as 54 Gy for 3-beams plans, 65.45 Gy for 5-beams plans and 73.64 Gy for 7-beams plans.

Structure	*Min/Max*	*Type*	*Goal*	*Priority*
GTV	Maximise (minimum)	Linear	A	Constraint
GTV	Minimise (maximum)	Linear	A*1.24	2
PTV	Maximise (minimum)	Linear	A*0.98	Constraint
PTV without GTV	Maximise (minimum)	Linear	A*0.96	Constraint
PTV without GTV	Minimise (maximum)	Linear	A*1.24	1
Spot overlap ROI	Minimise (maximum)	Quadratic	0	3
Shell 3 mm	Minimise (maximum)	Linear	A*0.62	4
Shell 3 mm	Minimise (maximum)	Mean	A*0.62	5
Shell 6 mm	Minimise (maximum)	Linear	A*0.31	6
Shell 6 mm	Minimise (maximum)	Mean	A*0.31	7
Shell 9 mm	Minimise (maximum)	Linear	0	8
Shell 9 mm	Minimise (maximum)	Mean	0	9
Shell 20 mm	Minimise (maximum)	Linear	0	10
Shell 20 mm	Minimise (maximum)	Mean	0	11
Outside of PTV	Minimise (maximum)	Linear	0	12
Outside of PTV	Minimise (maximum)	Linear	0	13
Outside of PTV	Minimise (maximum)	Mean	0	14
Lung ipsilateral without PTV	Minimise (maximum)	Linear	0	15
Lung ipsilateral without PTV	Minimise (maximum)	Mean	0	16
Lung other side	Minimise (maximum)	Linear	0	17
Lung other side	Minimise (maximum)	Mean	0	18
Oesophagus	Minimise (maximum)	Linear	31.5	Constraint
Oesophagus	Minimise (maximum)	Linear	0	19
Oesophagus	Minimise (maximum)	Mean	0	20
Spinal cord	Minimise (maximum)	Linear	21.6	Constraint
Spinal cord	Minimise (maximum)	Linear	0	21
Spinal cord	Minimise (maximum)	Mean	0	22
Trachea	Minimise (maximum)	Linear	36	Constraint
Trachea	Minimise (maximum)	Linear	0	23
Trachea	Minimise (maximum)	Mean	0	24
Bronchus ipsilateral	Minimise (maximum)	Linear	38.1	Constraint
Bronchus ipsilateral	Minimise (maximum)	Linear	0	25
MU	Minimise (maximum)	Linear	1	26

Appendix B. PBS delivery times

Table B1: Maximum PBS delivery time of treatment plans without spot overlap optimisation.

Patient	*Beam 1*	*Beam 2*	*Beam 3*	*Beam 4*	*Beam 5*	*Beam 6*	*Beam 7*
1	361.3	432.7	183.3				
2	224.2	246.8	224.7				
3	185.7	309.3	251.6				
4	176.1	274.9	143.6				
5	314.5	214.0	209.5				
6	247.4	131.4	122.7				
1	266.0	258.9	193.5	224.4	244.6		
2	184.2	143.0	137.6	153.6	171.7		
3	168.1	186.3	174.6	222.2	205.0		
4	144.2	178.0	142.1	132.4	137.4		
5	167.4	162.5	172.0	170.6	201.3		
6	121.2	111.1	118.0	96.6	122.9		
1	249.7	148.4	239.0	139.0	173.2	209.6	148.4
2	129.2	143.6	147.1	105.4	114.8	104.2	132.3
3	129.6	173.4	161.1	153.7	166.0	155.6	135.6
4	121.3	150.9	88.5	108.6	101.3	89.3	99.6
5	128.7	140.6	122.6	136.9	132.9	160.8	173.5
6	85.0	102.5	104.4	93.7	89.7	63.6	94.2

Table B2: mean PBS delivery time of PBS delivery time of treatment plans without spot overlap optimisation.

Patient	*Beam 1*	*Beam 2*	*Beam 3*	*Beam 4*	*Beam 5*	*Beam 6*	*Beam 7*
1	132.1	166.3	68.5				
2	89.9	95.3	110.0				
3	70.2	135.3	94.5				
4	69.5	114.1	67.2				
5	122.4	82.6	77.5				
6	99.9	70.5	66.5				
1	102.5	93.8	83.8	81.1	93.2		
2	72.7	74.7	54.4	71.2	67.6		
3	64.6	69.7	71.1	86.8	75.9		
4	58.0	73.4	51.4	53.6	52.5		
5	70.5	62.5	66.6	64.7	78.9		
6	56.1	63.1	51.7	57.8	65.3		
1	90.4	62.0	91.5	60.2	64.2	79.1	64.6
2	50.7	61.0	68.7	40.4	52.0	55.6	49.4
3	51.3	66.6	60.3	58.1	64.2	51.6	53.7
4	47.9	62.7	34.7	44.4	39.9	39.4	38.8
5	52.2	52.5	47.4	51.0	53.3	61.3	64.6
6	37.8	56.5	58.0	40.7	42.2	39.1	48.7

Table B3: Maximum travel times as part of PBS delivery time for all treatment plans without spot overlap optimisation.

Patient	*Beam 1*	*Beam 2*	*Beam 3*	*Beam 4*	*Beam 5*	*Beam 6*	*Beam 7*
1	24.8	23.6	15.6				
2	12.4	12.8	8.8				
3	14	19.2	17.6				
4	13.2	16.4	8.8				
5	16	13.6	16.4				
6	9.6	8.4	6.8				
1	21.6	20	18.4	16	18		
2	10.8	8	10	8	12.4		
3	14.8	14.4	16	13.6	16.4		
4	11.2	10	11.6	9.6	8.4		
5	14.4	11.2	12.8	12	12		
6	8.4	6	7.6	3.6	6.4		
1	6.4	6	5.6	6.4	7.2	2.8	5.6
2	9.6	9.6	9.6	10.4	9.6	4.4	6.4
3	10.4	9.2	7.2	10	7.6	4.4	10
4	12.8	13.2	10.8	12.8	12.4	13.2	12
5	19.6	17.2	19.2	16.8	13.2	16.8	16
6	12	9.6	9.2	11.2	12.4	11.2	12.4

Table B4: Maximum PBS delivery time of all treatment plans with full-plan spot overlap minimisation.

Patient	*Beam 1*	*Beam 2*	*Beam 3*	*Beam 4*	*Beam 5*	*Beam 6*	*Beam 7*
1	365.1	406.8	206.0				
2	254.9	245.8	299.3				
3	194.7	311.3	249.4				
4	356.7	296.8	18.7				
5	381.4	144.0	188.3				
6	380.3	114.4	84.2				
1	384.3	242.7	275.8	236.5	136.3		
2	210.7	89.0	187.9	178.0	160.5		
3	161.1	185.6	186.0	236.6	184.5		
4	164.1	220.2	145.4	152.0	200.1		
5	201.0	65.1	372.0	171.5	191.6		
6	146.1	130.6	125.6	79.4	90.5		
1	185.7	192.5	175.6	209.1	189.9	253.8	154.2
2	99.2	229.7	99.1	177.4	117.4	50.6	177.5
3	135.4	145.4	143.7	138.0	178.4	172.4	140.3
4	91.7	157.4	123.4	175.4	181.6	72.9	155.5
5	85.6	117.5	92.4	154.3	203.2	207.0	155.1
6	108.7	77.4	68.6	121.3	140.8	168.9	103.3

Table A5: Mean PBS delivery time of all treatment plans with full-plan spot overlap minimisation.

Patient	*Beam 1*	*Beam 2*	*Beam 3*	*Beam 4*	*Beam 5*	*Beam 6*	*Beam 7*
1	135.3	153.5	77.4				
2	94.9	93.2	120.5				
3	74.7	135.2	88.9				
4	143.1	112.3	8.3				
5	149.9	57.0	72.0				
6	148.0	57.9	45.9				
1	144.2	92.1	112.1	82.3	42.3		
2	74.2	51.5	71.4	66.7	61.0		
3	63.1	68.4	75.2	91.2	67.9		
4	67.2	81.0	54.5	62.5	74.3		
5	72.2	25.2	137.3	64.7	65.5		
6	61.5	76.1	54.0	45.8	48.4		
1	63.0	71.1	66.2	85.2	70.2	97.1	66.8
2	34.9	88.8	50.6	62.5	46.4	34.6	66.6
3	56.3	48.9	49.9	53.3	68.1	58.8	60.7
4	33.1	57.0	44.8	74.9	65.1	36.9	65.9
5	35.1	40.6	31.4	61.6	77.7	80.1	60.2
6	44.5	37.4	32.2	48.7	63.6	89.7	46.1

Table B6: Maximum travel times as part of PBS delivery time for all treatment plans with full-plan spot overlap minimisation.

Patient	*Beam 1*	*Beam 2*	*Beam 3*	*Beam 4*	*Beam 5*	*Beam 6*	*Beam 7*
1	24.8	24	20				
2	31.6	37.2	54.8				
3	14	17.2	14.8				
4	10.4	7.6	2				
5	14.4	6.4	11.2				
6	7.6	3.6	2.4				
1	16	13.2	15.2	7.2	9.6		
2	9.6	4	9.2	7.2	10.4		
3	13.2	13.2	15.6	14.4	14.8		
4	30.8	31.2	35.2	34.4	46		
5	7.2	2.4	8	7.6	7.6		
6	6.4	4	5.2	2	3.2		
1	16	18	15.2	14	11.2	14	14.4
2	5.2	7.6	2.8	6.8	3.6	0.8	9.2
3	10	9.2	6.8	9.2	12	11.2	12
4	6.4	6	6	8.4	6.4	1.6	6
5	6.4	5.2	4.8	8	9.2	8.8	9.2
6	5.2	2.4	2.8	6.8	4.4	3.6	2.4

Appendix C: Patient 6, 7-beams plan case

This is the case containing the lowest PBS delivery times. Optimisation of this treatment plan is done without overlap minimisation. The plan contains Bragg peaks inside healthy tissue and is therefore not clinically acceptable in its current state.

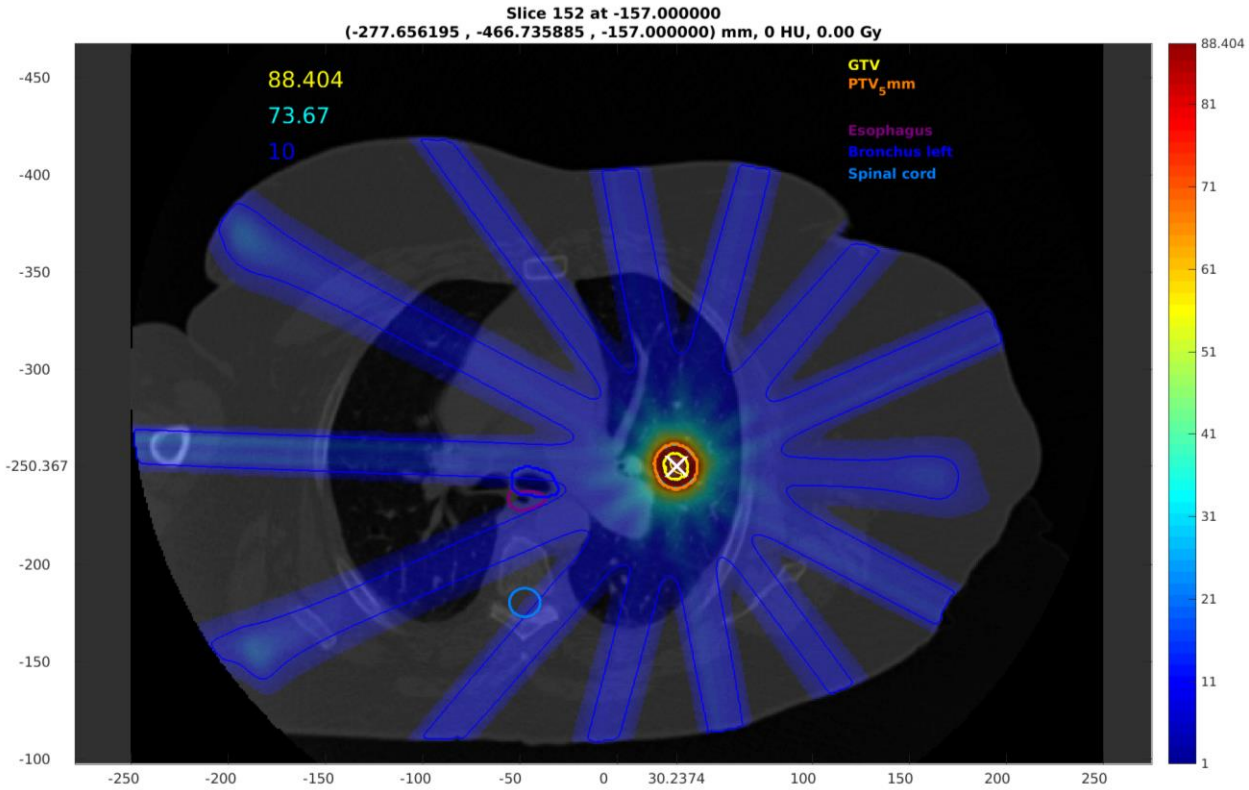

Figure C1: Dose distribution of the 7-beams plan of patient 6 without spot overlap optimisation. The PTV is shown with an orange border line, oesophagus with purple, ipsilateral bronchus with dark blue and the spinal cord is shown in light blue. The 10 Gy isodose line is dark blue and the isodose line equal to the target dose is (when visible) light blue. Beam 2, 3 and 6 contain a bragg peak inside the patient of which beam 2 and 3 are close to the skin.

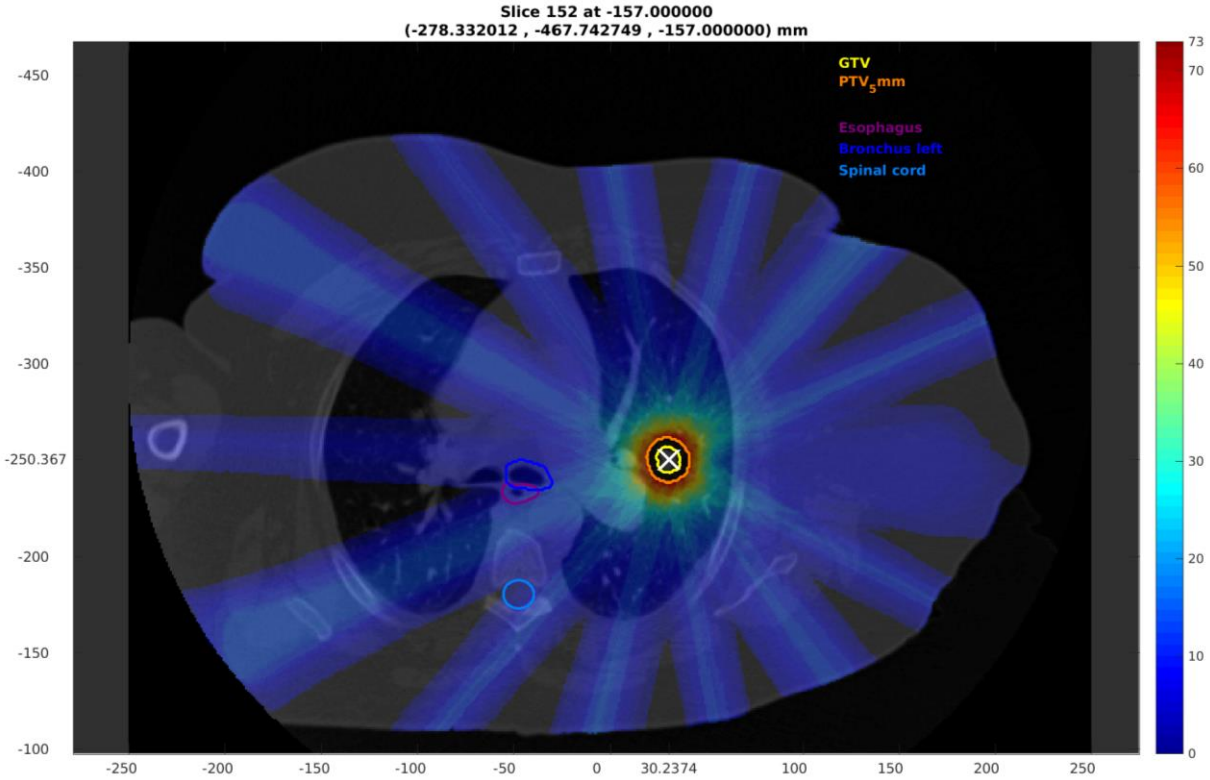

Figure C2: Spot-overlap distribution of the 7-beams plan of patient 6. No spot overlap optimisation used. The PTV is shown with an orange border line, oesophagus with purple, ipsilateral bronchus with dark blue and the spinal cord is shown in light blue.

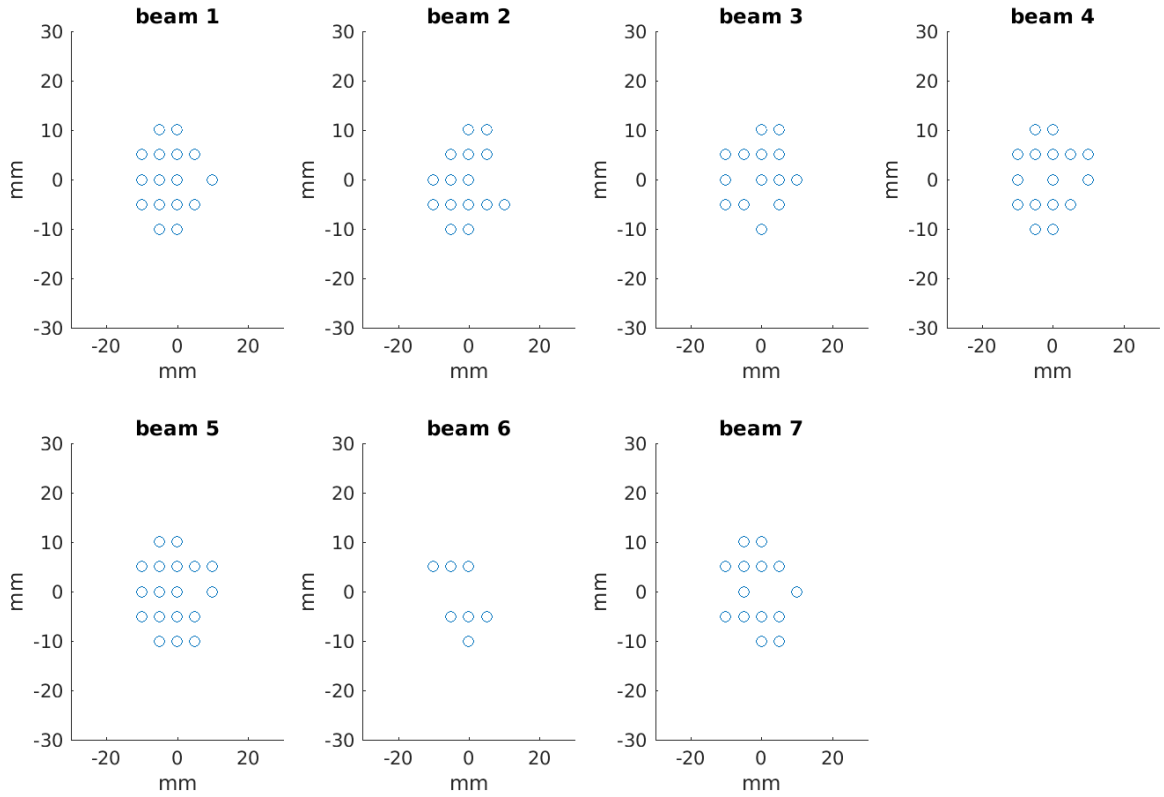

Figure C3: Pencil-beam (Spot) distributions per beam of the 7-beam plan of patient 6. No spot-overlap optimisation used. Beam 6 has significantly less spots. This beam is the beam covering the longest distance within the patient.

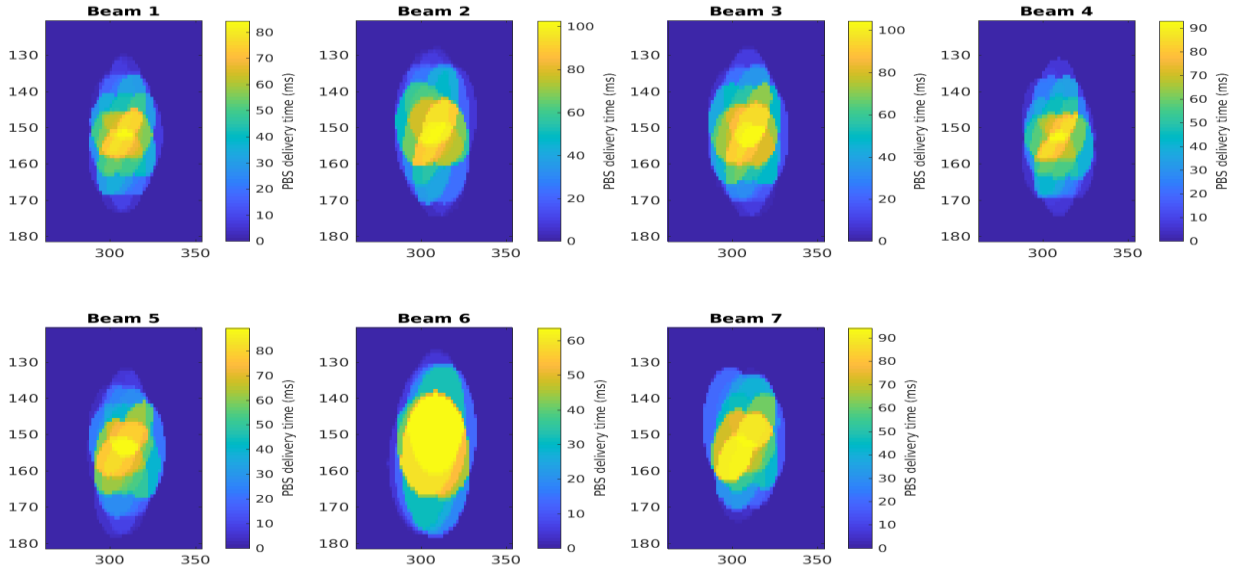

Figure C4: PBS delivery-time distributions per beam of the 7-beams plan of patient 6, not optimised on delivery time. Almost all areas can be delivered within 100ms.

Appendix D: Literature study

Erasmus University Medical Center, department of radiotherapy

-

Delft University of Technology

How to optimise FLASH in clinical IMPT treatment planning

Literature review and recommendations for optimisation and evaluation of stereotactic lung treatment with proton transmission beams

MSc Literature study

Author:
J. Groen
4618378

Supervisor Erasmus University Medical Center:
Dr S.J.M. Habraken

Supervisor Delft University of Technology:
Dr Ir. D. Lathouwers

April 25, 2020

Abstract

The treatment of malignant tumours using radiotherapy has improved significantly over the past decades. However, as irradiation of healthy tissue is unavoidable, side effects of radiotherapy, that is, healthy tissue toxicity, remain a problem. In addition to fractionation and online image-guidance, FLASH-radiotherapy, i.e. radiotherapy using very-high dose-rates, could be a third way of substantially improving the therapeutic window.
Lately, research around FLASH has been on a rise, and its existence can no longer be ignored. However, despite several attempts, the mechanics behind the effect have not yet been resolved. Nevertheless, clinical trials on FLASH are an upcoming step in the near future.
Pursuing FLASH radiotherapy for lung tumours using pencil beam scanning proton irradiation, FLASH treatment plan optimisation is necessary. Although state-of-the-art clinical cyclotrons are able to deliver the required dose-rates, the impact of PBS on FLASH is potentially negative and needs to be taken into account. Furthermore, due to the lack of understanding of the underlying mechanisms of FLASH, direct optimisation of FLASH is not feasible. However, FLASH indicators such as dose-rate, total irradiation time, dose-averaged dose-rate, beam overlap and spot overlap provide useful handholds for evaluation of FLASH treatment plans. For the optimisation of these, treatment plans containing 3 to 7 proton transmission beams at maximum cyclotron energy are a good starting point.

Preface

This report is written within the framework of a master thesis project conducted by Jort Groen, master student Biomedical engineering at the Delft University of Technology, The Netherlands.
This project is commissioned by the Erasmus Medical Centre, Rotterdam, The Netherlands. "The Erasmus MC encompasses a full spectrum of clinical services, including those provided by two specialist units operating under the Erasmus MC umbrella: the Erasmus MC Sophia Children's Hospital and the Erasmus MC Cancer Institute. Both have unique reputations of their own in the world of university hospitals." [1].
I would like to thank everybody, who in his/her way contributed to this internship. In particular, I would like to thank my supervisors from the Erasmus MC, Steven Habraken, Sebastiaan Breedveld and Mischa Hoogeman, for coaching me weekly, helping me with technical problems and providing support during writing. Furthermore, I would like to thank my supervisor from the TU Delft, Danny Lathouwers, for his support during this project.

Table of Contents

1 Introduction

Treatment of cancer is often done using a combination of three primary modalities. Surgery as a local treatment, radiotherapy for local-regional control and chemotherapy for systemic disease. Additionally, relatively new systemic modalities such as immunotherapy and hormonotherapy are being used in the fight against cancer. Over the past decades, radiotherapy (RT) has improved significantly, increasing its therapeutic window. New technologies such as online imaging (CBCT, MRI-linac) and more precise irradiation techniques (Cyberknife, proton therapy) make radiotherapy more accurate than ever. However, the side effects of irradiation due to healthy tissue toxicity are inevitable for even the most sophisticated techniques and often limits the capabilities of RT, restraining its curative potential and reducing patient quality of life. Irradiation of healthy tissue is inevitable due to (I) unavoidable entry doses, (ii) the infiltration of tumours in healthy tissue that therewith become part of the clinical target volume (CTV) and (iii) even the most precise techniques need robustness margins on the CTV/PTV to ensure tumour coverage and hereby control. Recently, developments around the so-called "FLASH effect" are on the rise. FLASH is a biological effect found when irradiating at very-high dose-rates in combination with short irradiation times and introduces additional sparing of healthy tissue [2]–[13]. The FLASH effect has been shown to benefit a variety of different tissues and organs in cell and animal models, e.g. intestine [10], [13], brain [3], [7], [8], skin [4] and lung [6], [12]. The FLASH effect can substantially widen the (intrinsic) therapeutic window of radiotherapy since (I) the irradiation of healthy tissue is unavoidable and (ii) organs at risk are becoming more frequently dose-limiting clinical practice. FLASH-RT is, therefore, a promising technique worth further investigation for clinical use. In addition, FLASH irradiation will have other advantages, e.g. shorter treatment times can enable higher patient flow-through and techniques such as breath-holding, of which the latter reduces the effects of organ movement and therefore could allow for smaller margins.

1.1. The FLASH effect

FLASH radiotherapy involves irradiating a patient using very-high (>40 Gy/s) mean dose-rates in combination with short irradiation time (<100ms) compared to conventional dose rates (~0.01 Gy/s) with treatment times in the order of minutes. The potential healthy tissue benefits from high dose-rate treatment were first found for intestine and skin toxicity [14]–[17]. Although multiple studies found similar effects, FLASH was never clinically implemented as it was unfeasible with radiotherapy equipment at that time. Healthy tissue doses would have been too high, the effect was assumed to be disadvantageous for tumour control (although no actual tumour study had been done) and the required techniques to generate such high dose-rates were not or barely available [18]–[20].
In 2014, Favaudon *et al.* re-observed the FLASH effect when investigating lung fibrogenesis in mice [2]. After this, several animal studies have been performed on, e.g. mice brain function [3], [5], [7], [8], mice lung fibrosis [2], [12], mice intestine injury and function [10], [13], mini-pig skin response and cat squamous cell carcinoma control [4], all confirming the FLASH effect. Furthermore, the first human patient was recently treated using FLASH-RT [9] for a superficial lesion of a recurrent sarcoma. Additionally, multiple in vitro studies have been performed, aiming to uncover the mechanics behind the effect [6], [11]. Possible mechanisms hypothesised include radiolytic oxygen depletion, change in redox metabolism, reduced damage to circulating immune system cells and chromatin remodelling [21]–[23]. However, not all studies investigating irradiation using very high dose-rates have found the effect [24]–[28]. Furthermore, the studies that did find a FLASH effect suggest high dose rates alone are not sufficient for the effect to occur, and other delivery restrictions apply.

Focussing on the area of lung cancer, the study performed by Favaudon *et al*. [2] found a significant reduction in complications and additional sparing of healthy smooth muscle and epithelial cells from acute radiation-induced apoptosis while remaining similar tumour control. Under these conditions, a dose-modifying factor was estimated to be as high as 1.8 [2]. In other words, similar healthy tissue responses were found for a dose that was 1.8 times higher when using FLASH irradiation with respect to conventional irradiation. Aside from this, the acute and long-term biological effects of high dose-rates have been investigated in human lung fibroblast cells by Buonanno *et al.* [6]. Ultra-high dose-rates reduced DNA damage, cell senescence and inflammatory responses. A similar conclusion was drawn by Fouillade *et al.* studying the effect of FLASH irradiation on mouse lung [12].

1.2. Problem definition

Although many experiments confirmed the FLASH beneficial effect, and even the first human patient has been treated, an optimal treatment planning strategy is still lacking. The development of such a strategy, combining FLASH with the dosimetric advantages of proton therapy with pencil beam scanning, is not straightforward since it is currently unclear under which conditions the FLASH effect can be expected.
This literature review aims to give an overview of current FLASH literature and thereby tries to identify (i) if and under what conditions a FLASH effect can be expected when irradiating using pencil beam scanning proton therapy, (ii) if treatment planning optimisation on FLASH is possible, (iii) what FLASH indicators and evaluators can be used for the FLASH optimisation and (iv) what is a good starting point for FLASH optimisation.
Within this review, special attention is given to FLASH for lung patients. These patients are of particular interest because (i) there is promising evidence from pre-clinical studies that a FLASH effect exists for lung tissue [2], [6], [12] and (ii) FLASH compatible dose-rates are the easiest to realise technologically in cyclotrons using transmission beams [29]. Although the use of transmission beams abolishes the distinctive effect of the protons “Bragg peak”, it is of benefit for lung-cancer patients since transmission beams mitigate range uncertainties and reduce movement uncertainties such as respiratory induced motion, a common problem when treating lung tumours. The advantage of this has already been shown by Mou *et al*. [30]

1.3. Literature search

Extensive search has been performed with the keywords: “FLASH radiotherapy”, “FLASH proton therapy”, “High dose-rate radiotherapy”, “High dose rate radiotherapy”, “Very-high dose-rate radiotherapy”, “very-high dose rate radiotherapy”, “Ultra-high dose rate radiotherapy” and “Ultra-high dose-rate radiotherapy”. Starting with these primary results, references from within these publications were also included.

2 Literature review

2.1. Mechanisms of FLASH

Although the biological mechanisms for conventional irradiation are well-understood, the underlying biological cause for the observed FLASH effect is still sparsely investigated. Conventionally, when irradiating using low LET radiation, complex DNA damage within cells generated mostly by double-strand breaks. Double-strand breaks are created both directly (33%) and indirectly (67%) [31]–[33]. The indirect damage is due to the formation of free radicals through ionization of water molecules. These free radicals lead to harmful chemical reactions within the cells that generate the damage observed. Oxygen plays a vital role in the formation of free radicals. The lack of oxygen is thereby related to reduced DNA damage and can be formulated by the oxygen enhancement ratio (OER) that describes the difference in radiosensitivity of anoxic compared to normoxic conditions. As opposed to FLASH, conventional dose-rates do not drain the oxygen fast enough for this to happen since the oxygen is replenished by diffusion from capillaries. Radiolytic oxygen depletion (ROD), changing the oxygen condition of cells, is proposed by several research groups as one of the possible mechanisms underlying the FLASH effect [2], [7], [11], [13], [34].
Alternatively, a theory is proposed based on the prolonged effects of high dose-rates on cells [22]. This theory is based on specific cell damage caused by the formation of reactive oxygen species and redox-active metals. Changes in redox metabolism can modify cell damage and are, therefore, seen as a possible candidate for explaining the FLASH effect. Furthermore, several studies have linked biological and physiological factors with FLASH, such as lower inflammatory responses [2]–[8], [12]. Other possible mechanisms include circulating immune cell sparing due to short irradiation times and chromatin remodelling [23].

2.1.1. Radiolytic oxygen depletion

Correlation between ROD and radioresistance on cells was already found in the 1960s and 1970s [15]–[19], [35], [36]. However, after the (re)discovery of additional tissue-sparing effects due to high dose-rates in 2014, the in vivo importance of oxygen on the FLASH effect was emphasized in a study on cognitive sparing in mice. First, additional cognitive sparing was demonstrated when using very-high (FLASH) dose-rates [3], [5]. Hereafter, a mechanistic investigation was performed where increased oxygen tension was created in the mouse brain using carbogen breathing [7]. The increased oxygen tension appeared to reverse the neuroprotective effects as was gained by using FLASH compatible irradiation, therewith supporting the theory on ROD. More recently, a study again found a strong relationship between oxygen and FLASH effect in vitro [11]. Here, a strong FLASH dependence on both oxygen tension and dose was found. In figure 1 can be seen that a FLASH effect is only found for oxygen concentration between 0 and 20 %.
Furthermore, the differential effect becomes more evident for higher doses. These findings are also in line with the ROD theory. Furthermore, FLASH research addresses and takes account of the possibility of radiolytic oxygen depletion as an explanation for the FLASH effect.

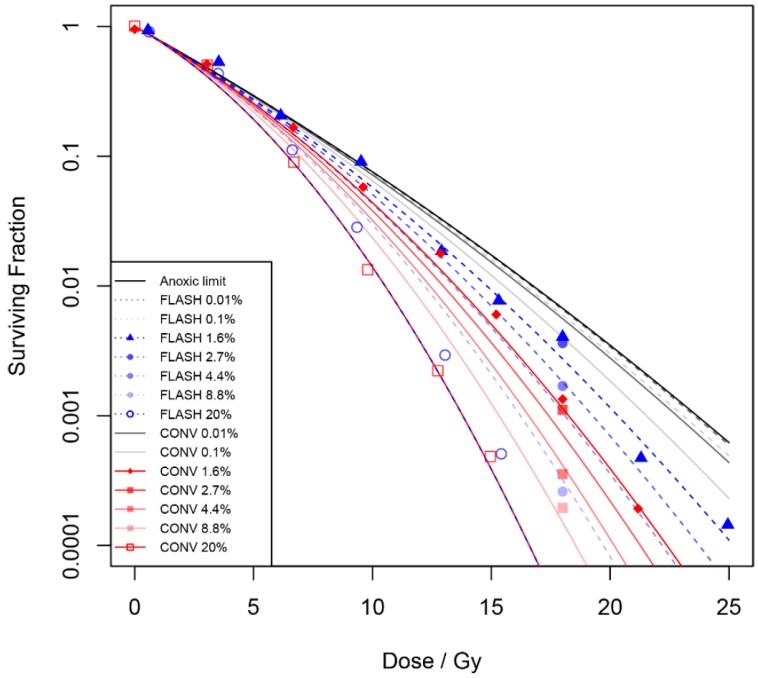

Figure 1: Figure taken from [11]. Relationship between survival fraction of prostate cancer cells, oxygen and dose. Surviving Fraction as a function of the dose given for FLASH and conventional irradiation. A differential FLASH effect is only apparent for oxygen concentrations between 0 and 20% and increases with dose. The data points are fitted using a Linear-quadratic fit.

Based on the ROD hypothesis, Pratx and Kapp argued that the effect of ROD on the OER could partially explain the FLASH effect [37]. When oxygen inside a cell is depleted, the hypoxic conditions result in decreased radiosensitivity as described by the decrease in OER, resulting in a protective effect. A visible representation of this is shown in figure 2, explaining the dependency of FLASH on both oxygen tension and dose. The delivered FLASH dose drains the oxygen within a cell and therewith “shifts” the OER curve to the left. This causes the cells to experience a lower OER and therewith reduced DNA damage. Using this assumption as a starting point, Pratx and Kapp designed two models describing the ROD theory for two cases: ultra-high dose-rates (>100 Gy/s) and very-high dose-rates (>10 Gy/s) [20]. Whereas the model for ultra-high dose-rates only considers tissue oxygen tension, the model for very-high dose-rates also takes oxygen diffusion and metabolic rate into account. The models can be found in appendix A.

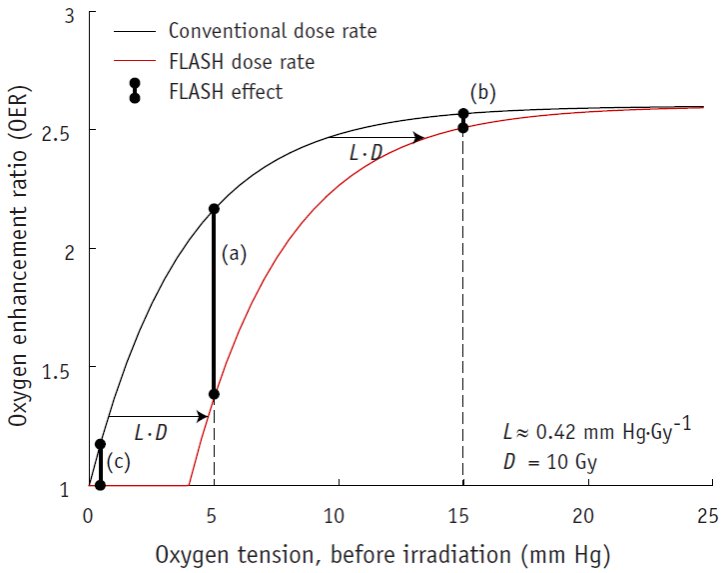

Figure 2: Figure taken from [37]. Visual representation of the gain in oxygen enhancement ratio as a function of oxygen tension. L ≈ 0.42 mm Hg/Gy is the oxygen depletion rate, D = 10 Gy is the dose delivered. The oxygen depletion as a result of irradiation is given by $L \cdot D$. Distances a, b and c visualise the gains in OER when using FLASH compared to conventional irradiation for oxygen tensions of 5, 15 and 1 mmHg respectively.

2.1.2. Other possible mechanisms

In addition to the theory based on ROD, other possible influences are hypothesised. Spitz *et al.* believe there might be a role of redox metabolism [22]. Differences in steady-state Reactive oxygen species (ROS) levels and redox metals are found in tumours as compared to healthy tissue. These differences might impact redox metabolism during irradiation [38]–[41]. Spitz *et al.* [22], provide an elaborate physico-chemical analysis that could partially explain part of the extended therapeutic window as also observed in the in-vivo studies. The analysis states that, in contrast to healthy tissue, tumour tissue has a slower dissipation of organic hydroperoxides, created during irradiation. Although not visible during conventional irradiation, when using very-high dose-rates, this characteristic results in a significantly larger dissipation time for tumour tissue. Because of this, a larger amount of organic hydroperoxides is present for a prolonged period and causes more DNA damage. The differences in DNA damage between healthy and tumour tissue lead to an increased therapeutic window. A visual representation of the dissipation induced differential effect is provided in figure 3.

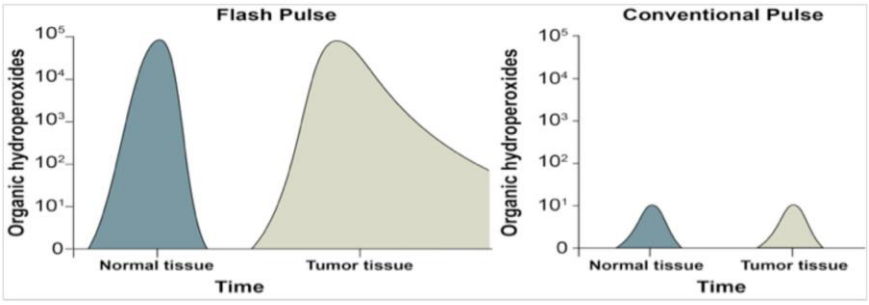

Figure 3: Figure taken from [22]. Differences in the dissipation of organic hydroperoxides in healthy vs tumour tissues for FLASH and conventional irradiation. Compared to healthy tissue, tumour cells take longer to completely dissipate all organic hydroperoxides after administering a very-high dose-rate pulse.

Other possible explanations for the FLASH effect indicate that the high dose-rate might influence delayed harmful effects. For example, chronic inflammatory responses may increase the risk of organ fibrosis [43], [44]. Furthermore, premature cell senescence could be a potential link between oxidative stress and prolonged tissue injury [45]. Senescent cells release pro-inflammatory molecules that have been found when investigating TGFβ [12], [43], [45]. It was therefore argued that dose-rate might affect long-term outcomes, triggered by an inflammatory response. Finally, other possible influences include circulating immune cell sparing due to short irradiation times and chromatin remodelling [23].

2.2. Irradiation delivery

The tissue sparing FLASH effect is expected to occur when irradiating using high dose-rates (>40 Gy/s) and low delivery times (<100ms). However, dose delivery has additional specifications that occasionally vary between different FLASH studies. For example, several studies used a pulsated electron beam with an energy between 4.5 and 20 MeV [2]–[4], [7]–[9], [11]–[13]. However, FLASH proton irradiations have been performed using cyclotrons (230 and 224 MeV) and singletron (4.5 MeV) [6], [10], [28]. In these studies, the FLASH effect was not always found [28]. In addition to electrons and protons, two photon high dose-rate experiments were conducted [5], [27]. In one of which no FLASH effect was observed [27]. Different delivery specifications per study are listed in appendix B. High-dose-rate experiments with long fraction times (in the order of minutes) are excluded from the table [24]–[26]. As can be expected from the long fraction times, these studies did not find a FLASH effect.

Most FLASH studies are done using a pulsed electron beam. Here, parameters such as dose-rate within the pulse, dose per pulse, pulse rate and pulse length result in different dose deliveries and might, therefore, influence the observed FLASH effect. Bourhis *et al. [34]* suggested that the most important parameters are:

- Fraction delivery time;
- Dose delivered in a single fraction;
- Mean dose-rate;
- Dose-rate within pulse

Unfortunately, one or more of these parameters are often not specified in reports on FLASH studies.
In addition to the parameters just stated, field size could also be a limiting factor [10]. This is based on the fact that larger field sizes require more flux to achieve FLASH compatible dose-rates. For example, for protons, a field of 5 cm x 5 cm, delivering 100 Gy/s would require a beam current of 600nA [10]. For pencil beam scanning, the delivery consists of a combination of smaller spots. The influence of this on FLASH has not yet been investigated.
Finally, the influence of high-LET radiation on FLASH has not been investigated as well. Current particle irradiation was done using sufficiently high energies so that dose delivery is done using the run-up of the dose deposition curve, considered to be low-LET irradiation.

2.3. Treatment planning

Recently, the first human patient received FLASH-RT for a 3.5 cm ulcero-infiltrating tumour on the right forearm [23]. This treatment consisted of a single fraction of 15 Gy from one beam. The dose was delivered in 10 pulses of 1μs, each uniformly distributed within 90ms. Given the size and position of the tumour, advanced treatment planning was unnecessary.
Although electron FLASH irradiation is, in its current form, only suitable for superficial tumours, deeper tumours can be irradiated using high energy protons. In those cases, more advanced treatment planning

is often necessary due to tumour shape and organs at risk close to the target. Aside from the larger range, better dose distributions are often achieved when using protons, leaving space for optimisation and spatial distribution of the FLASH effect.

For proton therapies delivered using pencil beam scanning (PBS), the setup usually consists of multiple beam angles, each divided into smaller pencil beams. This results in a wide range of tunable variables and possibilities conventionally used to optimise dose distribution. However, using this space to optimise not only dose distribution but also FLASH effect is not trivial. Van de Water *et al.* compared different treatment plan approaches and delivery methods for four head-and-neck patients to find potential FLASH treatment plan options [46]. For evaluation on FLASH, van de Water *et al.* proposed a dose-averaged dose-rate (DADR) as a measure for determining the average dose-rate. The DADR can, therefore, be used as a predictor of the FLASH effect. The DADR for each voxel inside a treatment plan is given as equation 1, modelled as in reference [46].

$$DADR_i = \sum_{j=1}^{n} \frac{d_{ij} \cdot \dot{d}_{ij}}{\sum_{k=1}^{n} d_{ik}} \qquad (1)$$

where:
DADR = dose-averaged dose-rate [Gy/s];
I = voxel;
j,k = pencil beam;
n = number of pencil beams;
d = dose-rate [Gy/s];
$\dot{d}$ = dose-influence matrix [Gy/proton];

Van de Water *et al.* concluded that FLASH dose-rates were only achieved when using increased spot-wise beam intensities, spot-reduced planning, hypofractionation and arc-shoot-through (transmission beam) plans [46].
Aside from this study, van Marlen *et al.* investigated dose-rate distributions and delivery times for FLASH proton transmission beam plans as an alternative for stereotactic lung irradiation [47]. For evaluation on FLASH, physical parameters, i.e. dose-rate distribution within a beam, overall irradiation time, number of tissue revisits and relative FLASH contribution were considered. Here, FLASH contribution at a particular voxel was defined as stated in equation 2, modelled as in reference [49].

$$F_i = \left(\sum_{j:\dot{d}_{ij} \geq 40} \frac{d_{ij}}{\sum_{k=1}^{n} d_{ik}} \right) \times 100\% \qquad (2)$$

where:
F = relative contribution of FLASH [%];
i = voxel;
j = pencil beam;
n = number of pencil beams
$\dot{d}$ = dose-rate [Gy/s]
d = dose [Gy];
$\dot{d}_{ij} \geq 40$ = pencil beam that deliver a dose to voxel i with a dose-rate more or equal to 40 Gy/s;

Clinical comparison of the FLASH plans was made with clinical volumetric-modulated arc therapy (VMAT) plans. In total, comparison and evaluation were made for 10 FLASH plans, based on 7 patients. All FLASH plans were non-coplanar and used 244 MeV (transmission) protons.
Using a dose-rate in the middle of the spot (SPDR) of 100 Gy/s, a FLASH contribution value of ~40% was achieved. For an SPDR of 360 Gy/s, this increased to 75%. Total irradiation time of the FLASH plans where between 300 and 730 ms. Van Marlen *et al.* suggests optimising plans on delivery time [47].

3 Discussion

3.1. FLASH effect in pencil beam scanning proton therapy for lung tumours

Many studies found a FLASH effect. However, the majority of these studies are performed by the French-Swiss research group. Furthermore, some of these studies are performed using only a few test subjects/volunteers. E.g. 1 mini-pig [4], 4 cats [4] or 1 human [9]. Therefore, it is not possible to unambiguously prove the existence of the effect using these results, and unravel the underlying mechanisms.
Most FLASH studies have been carried out using a single pulsed electron beam with energies between 4.5 and 16 MeV. Nevertheless, a FLASH effect has also been found for photon [5] and proton [6], [10] irradiation. Acceleration of protons has been done using a single millisecond pulse at energies of 4.5 [6], 230 [10] and 224 MeV [28]. However, in one case, the existence of a FLASH effect was not concluded [28]. A clear difference between the linac electron and cyclotron proton delivery is the pulsation in combination with extremely-high dose-rates. Even though the significance hereof has not yet been shown and a FLASH effect has been found for cyclotron delivery, creating such high instantaneous dose-rates using a cyclotron is unfeasible using current technology. However, following the ROD hypothesis, high dose-rates in combination with significant doses are needed to deplete the oxygen and thus invalidates the influence of pulsation. Following the models of Pratx and Kapp, a pulsated beam would be disadvantageous compared to a single pulse [21]. However, given the short overall irradiation time, the effect of the pulsation and corresponding extremely-high dose-rates would most likely not result in significantly different results compared to the same dose delivered within a single pulse over similar total irradiation time.
Another difference between the commonly used electrons and protons is the difference in LET. Because beamline transport is more efficient at higher energies [29] and no energy degraders are needed, higher dose-rates can be achieved using this setting. As a result, the Bragg peak will shift out of the patient and irradiation will be done using transmission beams and can therefore also be considered as low-LET radiation.
The proton study that could not conclude a FLASH effect [28] was a study on zebrafish embryo survival, very similar to one performed with electrons that did find a FLASH effect [7]. When investigating differences between the two studies, it can be seen that the total irradiation time used in the proton study is up to 400 ms, higher than the commonly assumed FLASH threshold of about 100 ms, whereas it was 150 ms for the electron study. Furthermore, Although the authors concluded no FLASH effect to be found, they did find a significant benefit for high dose-rates for a delivered dose of 23 Gy. Finally, the authors did state that the embryos have been kept in an aquatic medium during irradiation. Due to skin oxygen diffusion uptake, this could have influenced the oxygen depletion and thereby obstructed the FLASH effect [28].
In conclusion, FLASH effect can likely be recreated using cyclotron proton irradiation delivery using PBS.

3.2. Direct optimisation of the FLASH effect

Many studies have related the FLASH effect to oxygen depletion [2], [7], [11], [13], [22], [48]. In particular, clear relationships between oxygen tension, FLASH delivered dose, and increased surviving cell fraction has been found [11]. These in vitro results imply that the FLASH effect is dependent on ROD and could, therefore, be described by the models created by Pratx and Kapp [21]. This can be very useful when optimising treatment plans on FLASH. However, the models do not seem to describe in vivo results

accurately. For example, the relationship between tissue tension delivered FLASH dose and the relative decrease in radiosensitivity is shown in figure 4. As can be concluded from this figure, the model designed for ultra-high dose-rates (>100 Gy/s) shows a minimal decrease in radiosensitivity at higher tissue oxygen tensions. This contradicts studies that have shown a clear benefit due to FLASH in lung tissue [2], [6], [12], which is known to be very well oxygenated. For example, at lung tissue near the alveolar capillaries, only 1.3 % O_2 depletion would occur after 10 Gy irradiation [2(S2)]. According to the model, complete depletion in this tissue would require high doses (>100 Gy) for a decrease in radiosensitivity of only 10%. This does not correspond to the in vivo results found for lung tissue [2]. However, the idea that, in vitro, better-oxygenated tissues would require more dose for full oxygen depletion is not new. It is also used to explain the reduced modifying factors found for better-oxygenated tissues as summarised by Vozenin *et al.* [48] and also fits the findings of Adrian *et al.* [11].

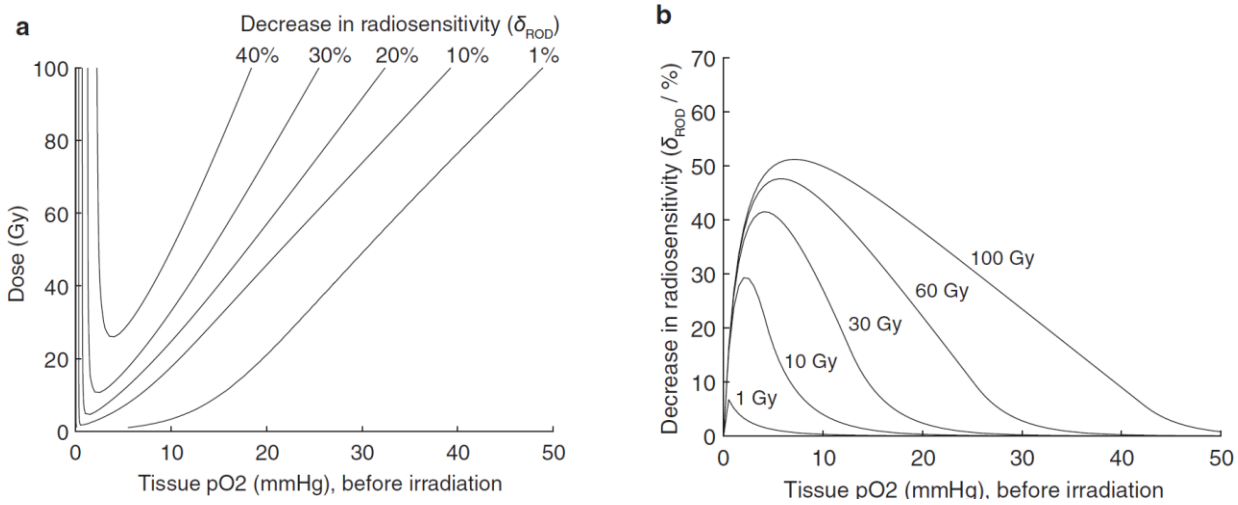

Figure 4: Figure taken from [21]. Relative decrease in radiosensitivity (δ_{ROD})due to ROD for ultra-high dose-rate (>100 Gy/s). (a) Relationship between FLASH dose delivered and tissue oxygen tension (partial pressure) for different δ_{ROD} objectives. (b) Same data, δ_{ROD} as a function of oxygen tension for different FLASH doses delivered.

Contrary to the first model, the model for very-high dose-rates (>10 Gy/s) shows that different oxygen tensions would merely shift the area receiving the FLASH benefit further away from the neighbouring capillary as oxygen tension decreases with distance from its nearest capillary. This can be concluded from figure 5, where the relative decrease in radiosensitivity is plotted against the distance from capillary for different oxygen tensions.

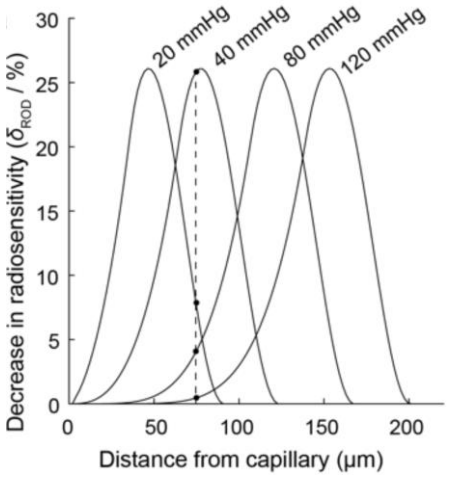

Figure 5: Figure taken from [21]. Relative decrease in radiosensitivity (δ_{ROD}) due to ROD for very-high dose-rate (>10 Gy/s). The δ_{ROD} is drawn as a function of distance away from capillary for different oxygen tensions. The reduction in radiosensitivity appears to be localised around a specific distance from the capillary, dependent on the tissue oxygen tension. An increase in oxygen tension results in a shift of the benefiting area away from the capillary.

Another interesting effect that can be derived from the model for very-high dose-rates is that only a fraction of the tissue receives a beneficial reduction in radiosensitivity, as can also be observed in figure 5. The question on to what extent FLASH is a local effect remains unanswered. Localization also does not seem to correspond with the in vivo literature as an overall healthy tissue sparing effect has always been found throughout the entire irradiated volume. However, it is hypothesised that the FLASH effect depends on the high dose-rate irradiation of hypoxic stem cell niches that could lead to the in vivo found results [58]. Nevertheless, considering the correspondence of the FLASH models with in vitro findings and the contradictions found with in vitro studies, it can be argued that there are more FLASH mechanisms which are either secondary effects resulting from the oxygen decrease and/or other (biological) effects caused by the short irradiation times and high dose-rates. Nevertheless, the descriptive models could give qualitative insight into the abundance of the FLASH effect in specific scenarios that can be useful for FLASH treatment plan optimisation. For example, the combination of high dose and dose-rates would be essential to deplete the oxygen and create additional sparing. This advocates for hypofractionation and dose-rate maximisation in high dose areas.
As a side note, if the ROD theory would be true, this implies that hypoxic tumour tissue will also benefit from FLASH irradiation. Therefore, one has to be careful with applying FLASH irradiation on hypoxic tumours.
One of the alternative theories, the physico-chemical approach based on differences in redox metabolism, can also help to explain the additional widening of the therapeutic window for FLASH. Compared to FLASH dose-rates, conventional dose-rate pulses would not produce sufficient free radicals and organic hydroperoxides fast enough to uncover these mechanisms. This implies that optimising a treatment plan based on dose-rate would help to maximise the FLASH effect. Other possible mechanisms such as circulating immune cell sparing would suggest minimisation of irradiation time. Further study is needed to verify whether and which of the proposed hypotheses are true and if so if this could describe the full FLASH effect as found in the in vivo studies.
For now, only for the ROD hypothesis, a model is available. Given the uncertainties on this model and the hypothesis as a whole, it is not advisable to perform optimisation solely based hereupon. Therefore, direct optimisation of FLASH is currently not possible. However, qualitative handgrips could be extracted from the models, i.e., optimisation based on dose-rate and total irradiation time, and the influence of multi pulsed irradiation can be used to guide towards FLASH optimisation.

3.3. FLASH effect indicators

In the clinic, treatment plans are evaluated on physical dose distribution. When attempting to take advantage of FLASH parameters, that is, average dose-rate and total irradiation time, need to be taken into account as well. In our case, very high energies are necessary to achieve FLASH dose-rates which results in transmission beam irradiation. Although this would remove the main advantage of particle therapy, namely the distinct Bragg peak, clinically acceptable plans have been generated with transmission beams and showed better FLASH potential compared to traditional photon treatment plans, currently used for radiotherapy of this cohort [46], [47], [49].
However, although these plans were considered clinically acceptable based on dose distribution and the instantaneous dose-rate is considered to be within FLASH regime, a FLASH effect cannot be assumed. Cell revisits from pencil beam scanning, and multiple beam angles can induce total irradiation times larger than the generally used FLASH irradiation time threshold of about 100 ms. Although the effect of cell revisits with interval times is in the order of milliseconds for PBS or seconds for beam angle rotation has not yet been identified, it can be expected that this potentially decreases the FLASH effect. Besides, when using PBS, some machines require a minimum pencil beam (spot) on-time. As a result, beam intensities are varied for spots with an irradiation time below this minimum [50]. Van de Water et al. proposed a 'dose-averaged dose-rate' (DADR) to assess the problem of PBS revisits and varying spot intensities. The DADR can be used to identify potential FLASH abundant and absence regions within the treatment plan [46]. In addition, we previously proposed spot and beam overlap as additional visualisations for identifying FLASH abundant and FLASH absent regions [51]. Whether DADR, spot or beam overlap can be utilised and is suitable for FLASH optimisation remains unknown.
The FLASH contribution, as proposed by van Marlen *et al.* [47], also suffers from the tissue revisit problem. Furthermore, the impact of spots delivering lower dose-rates at voxels is also not taken into account even though this dramatically decreases the average dose-rate. This metric is, therefore, unsuitable for evaluating the FLASH potential.
Within the Varian FlashForward consortium, the pencil beam scanning dose-rate has been proposed as an alternative evaluation metric. This quantity is defined as the dose delivered to a voxel, divided by the time interval between delivery the first pencil beam contributing a dose exceeding 0.01 Gy to that voxel, and the last pencil beam exceeding the same dose. A visual representation of the interval time is given in figure 6. Although the threshold value (<<b/a) is somewhat arbitrary, this measure does do justice to both dose and delivery time being relevant parameters.

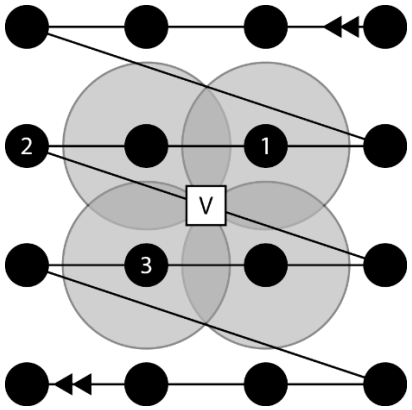

Figure 6: Illustration of pencil beam scanning dose-rate time interval on a rectangular grid for voxel ‘V’. During PBS, the first pencil beam delivering a dose exceeding 0.01 Gy at voxel V is denoted by ‘1’. The last pencil beam contributing more than 0.01 Gy to ‘V’ is denoted by ‘3’. Pencil beam 2 does not contribute dose to ‘V’. However, since the spot is delivered between the first and last spot, the spot delivery time still contributes to the time interval.

At last, it is important to note that a FLASH effect is not to be expected throughout the whole irradiated volume even if all irradiation is done with sufficient dose-rate and within FLASH irradiation times. Namely, the FLASH effect seems to only appear in tissues that receive sufficient dose. From all dose escalation studies done, it was found that the FLASH effect was more prominent at higher delivered doses with a minimum dose threshold often found at approximately 10 Gy [2], [4], [6], [11]. This finding is also in agreement with the oxygen depletion theory that states that a certain amount of dose needs to be delivered to deplete oxygen. In the clinic, this would mean that in a treatment plan, tissue-sparing effects due to FLASH will probably only occur at areas receiving higher doses such as area adjacent to the PTV. Because of the relatively high dose delivered in this tissue, this region is often dose-limiting. Therefore, additional sparing would also be most welcome here. The importance of sufficient dose advocates for hypofractionation, which is also found to improve some of the dose-rate and DADR indicators [46].
In conclusion, it is essential to look at multiple indicators when evaluating FLASH suitable treatment plans. The most important FLASH indicators are high dose regions, low spot overlap (few spot revisits), low beam overlap (few beam-revisits), high dose-rate regions and low total irradiation time.

3.4. A starting point for FLASH treatment plan optimisation

Proton transmission beams are to be used to achieve FLASH-compatible dose rates from a cyclotron. P. Cruijssen showed that clinically acceptable plans are possible using as few as 5 transmission beams [49]. This reduces cell revisits induced by multiple beam angles and therewith decreases the possibility of FLASH effect loss due to these revisits. Although it is unknown if this reduction of revisits is sufficient nor if cell revisits with intervals in the order of seconds would reduce or diminish the FLASH effect at all, It can be expected to do so. The number of possible beam angles, spot positions and spot intensities give rise to enormous freedom that can be tweaked in to balance physical dose distribution and FLASH potential. Treatment plans using 5 transmission beams are therefore a good starting point for optimisation of the FLASH potential.
Finally, whether or not a FLASH tissue sparing effect will be found, FLASH therapy allows shorter irradiation times. This can help mitigate uncertainties due to organ movement and reduces fraction treatment time. The latter benefits patient flow and could enlarge treatment capacity and enable cheaper treatment for more patients.

4 Conclusions

Feasibility of FLASH proton therapy for lung tumours is shown for cyclotron pencil beam scanning delivery. The high dose-rates required for FLASH-RT can be achieved using transmission beams. However, FLASH treatment plan optimisation is not trivial. The impact of multiple beam angles and PBS is unknown and likely affects the FLASH potential negatively. Although several attempts have been made on discovering the mechanics behind FLASH and a model was created based on the ROD theory, the lack of fundamental understanding makes direct optimisation of FLASH impossible. Nevertheless, FLASH indicators can be extracted from current literature that can help in evaluating treatment plans on FLASH potential and tested in near-future clinical trials. Promising indicators that relate to expected FLASH effect are high dose and dose-rate, short fraction irradiation time, high dose-averaged dose-rate, low beam overlap, and low spot overlap. These indicators can be used for quantitative insight when optimising the FLASH effect within a treatment plan. To stay on the save side, FLASH can be expected for doses higher than 10 Gy, dose-rates starting from 100 Gy/s and irradiation times of maximum 100 milliseconds. A good starting point for generating FLASH treatment plans are plans containing 5 transmission beams.

5 References

[1] 'The Erasmus MC Cancer Institute'. https://www.erasmusmc.nl/en/patient-care/about-erasmus-mc (accessed Jan. 27, 2020).

[2] V. Favaudon *et al.*, 'Ultrahigh dose-rate FLASH irradiation increases the differential response between normal and tumor tissue in mice', *Sci. Transl. Med.*, vol. 6, no. 245, pp. 245ra93-245ra93, Jul. 2014, doi: 10.1126/scitranslmed.3008973.

[3] P. Montay-Gruel *et al.*, 'Irradiation in a flash: Unique sparing of memory in mice after whole brain irradiation with dose rates above 100 Gy/s', *Radiotherapy and Oncology*, vol. 124, no. 3, pp. 365–369, Sep. 2017, doi: 10.1016/j.radonc.2017.05.003.

[4] M.-C. Vozenin *et al.*, 'The Advantage of FLASH Radiotherapy Confirmed in Mini-pig and Cat-cancer Patients', *Clin Cancer Res*, vol. 25, no. 1, pp. 35–42, Jan. 2019, doi: 10.1158/1078-0432.CCR-17-3375.

[5] P. Montay-Gruel *et al.*, 'X-rays can trigger the FLASH effect: Ultra-high dose-rate synchrotron light source prevents normal brain injury after whole brain irradiation in mice', *Radiotherapy and Oncology*, vol. 129, no. 3, pp. 582–588, Dec. 2018, doi: 10.1016/j.radonc.2018.08.016.

[6] M. Buonanno, V. Grilj, and D. J. Brenner, 'Biological effects in normal cells exposed to FLASH dose rate protons', *Radiotherapy and Oncology*, vol. 139, pp. 51–55, Oct. 2019, doi: 10.1016/j.radonc.2019.02.009.

[7] P. Montay-Gruel *et al.*, 'Long-term neurocognitive benefits of FLASH radiotherapy driven by reduced reactive oxygen species', *Proc Natl Acad Sci USA*, vol. 116, no. 22, pp. 10943–10951, May 2019, doi: 10.1073/pnas.1901777116.

[8] D. A. Simmons *et al.*, 'Reduced cognitive deficits after FLASH irradiation of whole mouse brain are associated with less hippocampal dendritic spine loss and neuroinflammation', *Radiotherapy and Oncology*, vol. 139, pp. 4–10, Oct. 2019, doi: 10.1016/j.radonc.2019.06.006.

[9] J. Bourhis *et al.*, 'Treatment of a first patient with FLASH-radiotherapy', *Radiotherapy and Oncology*, vol. 139, pp. 18–22, Oct. 2019, doi: 10.1016/j.radonc.2019.06.019.

[10] E. S. Diffenderfer *et al.*, 'Design, Implementation, and in Vivo Validation of a Novel Proton FLASH Radiation Therapy System', *International Journal of Radiation Oncology*Biology*Physics*, vol. 106, no. 2, pp. 440–448, Feb. 2020, doi: 10.1016/j.ijrobp.2019.10.049.

[11] G. Adrian, E. Konradsson, M. Lempart, S. Bäck, C. Ceberg, and K. Petersson, 'The FLASH effect depends on oxygen concentration', *Br J Radiol*, vol. 93, no. 1106, p. 20190702, Feb. 2020, doi: 10.1259/bjr.20190702.

[12] C. Fouillade *et al.*, 'FLASH Irradiation Spares Lung Progenitor Cells and Limits the Incidence of Radio-induced Senescence', *Clin Cancer Res*, pp. 1078-0432.CCR-19–1440, Dec. 2019, doi: 10.1158/1078-0432.CCR-19-1440.

[13] K. Levy *et al.*, 'FLASH irradiation enhances the therapeutic index of abdominal radiotherapy in mice', Cancer Biology, preprint, Dec. 2019. doi: 10.1101/2019.12.12.873414.

[14] S. Hornsey and T. Alper, 'Unexpected Dose-rate Effect in the Killing of Mice by Radiation', *Nature*, vol. 210, no. 5032, pp. 212–213, Apr. 1966, doi: 10.1038/210212a0.

[15] S. B. Field and D. K. Bewley, 'Effects of Dose-rate on the Radiation Response of Rat Skin', *International Journal of Radiation Biology and Related Studies in Physics, Chemistry and Medicine*, vol. 26, no. 3, pp. 259–267, Jan. 1974, doi: 10.1080/09553007414551221.

[16] S. Hornsey and D. K. Bewley, 'Hypoxia in Mouse Intestine Induced by Electron Irradiation at High Dose-rates', *International Journal of Radiation Biology and Related Studies in Physics, Chemistry and Medicine*, vol. 19, no. 5, pp. 479–483, Jan. 1971, doi: 10.1080/09553007114550611.

[17] J. H. Hendry, J. V. Moore, B. W. Hodgson, and J. P. Keene, 'The Constant Low Oxygen Concentration in All the Target Cells for Mouse Tail Radionecrosis', *Radiation Research*, vol. 92, no. 1, p. 172, Oct. 1982, doi: 10.2307/3575852.
[18] R. J. Berry and J. B. H. Stedeford, 'Reproductive survival of mammalian cells after irradiation at ultra-high dose-rates: further observations and their importance for radiotherapy', *BJR*, vol. 45, no. 531, pp. 171–177, Mar. 1972, doi: 10.1259/0007-1285-45-531-171.
[19] R. J. Berry, 'EFFECTS OF RADIATION DOSE-RATE: From Protracted, Continuous Irradiation to Ultra-High Dose-Rates from Pulsed Accelerators', *British Medical Bulletin*, vol. 29, no. 1, pp. 44–47, Jan. 1973, doi: 10.1093/oxfordjournals.bmb.a070955.
[20] E. J. Hall and D. J. Brenner, 'The dose-rate effect revisited: radiobiological considerations of importance in radiotherapy', *Int. J. Radiat. Oncol. Biol. Phys.*, vol. 21, no. 6, pp. 1403–1414, Nov. 1991, doi: 10.1016/0360-3016(91)90314-t.
[21] G. Pratx and D. S. Kapp, 'A computational model of radiolytic oxygen depletion during FLASH irradiation and its effect on the oxygen enhancement ratio', *Phys. Med. Biol.*, vol. 64, no. 18, p. 185005, Sep. 2019, doi: 10.1088/1361-6560/ab3769.
[22] D. R. Spitz *et al.*, 'An integrated physico-chemical approach for explaining the differential impact of FLASH versus conventional dose rate irradiation on cancer and normal tissue responses', *Radiother Oncol*, vol. 139, pp. 23–27, 2019, doi: 10.1016/j.radonc.2019.03.028.
[23] M. Durante, E. Bräuer-Krisch, and M. Hill, 'Faster and safer? FLASH ultra-high dose rate in radiotherapy', *Br J Radiol*, vol. 91, no. 1082, Feb. 2018, doi: 10.1259/bjr.20170628.
[24] C. Greubel *et al.*, 'Scanning irradiation device for mice in vivo with pulsed and continuous proton beams', *Radiat Environ Biophys*, vol. 50, no. 3, pp. 339–344, Aug. 2011, doi: 10.1007/s00411-011-0365-x.
[25] S. Auer *et al.*, 'Survival of tumor cells after proton irradiation with ultra-high dose rates', *Radiat Oncol*, vol. 6, no. 1, p. 139, 2011, doi: 10.1186/1748-717X-6-139.
[26] O. Zlobinskaya *et al.*, 'The Effects of Ultra-High Dose Rate Proton Irradiation on Growth Delay in the Treatment of Human Tumor Xenografts in Nude Mice', *Radiation Research*, vol. 181, no. 2, pp. 177–183, Feb. 2014, doi: 10.1667/RR13464.1.
[27] L. M. L. Smyth *et al.*, 'Comparative toxicity of synchrotron and conventional radiation therapy based on total and partial body irradiation in a murine model', *Sci Rep*, vol. 8, no. 1, p. 12044, Dec. 2018, doi: 10.1038/s41598-018-30543-1.
[28] E. Beyreuther *et al.*, 'Feasibility of proton FLASH effect tested by zebrafish embryo irradiation', *Radiotherapy and Oncology*, vol. 139, pp. 46–50, Oct. 2019, doi: 10.1016/j.radonc.2019.06.024.
[29] U. W. Langner, J. G. Eley, L. Dong, and K. Langen, 'Comparison of multi-institutional Varian ProBeam pencil beam scanning proton beam commissioning data', *J Appl Clin Med Phys*, vol. 18, no. 3, pp. 96–107, May 2017, doi: 10.1002/acm2.12078.
[30] B. Mou, C. J. Beltran, S. S. Park, K. R. Olivier, and K. M. Furutani, 'Feasibility of Proton Transmission-Beam Stereotactic Ablative Radiotherapy versus Photon Stereotactic Ablative Radiotherapy for Lung Tumors: A Dosimetric and Feasibility Study', *PLoS One*, vol. 9, no. 6, Jun. 2014, doi: 10.1371/journal.pone.0098621.
[31] F. Hutchinson, 'Radiation Biochemistry. Volume 1: Cells. Shigefumi Okada , Kurt I. Altman , Georg B. Gerber Molecular Radiation Biology. The Action of Ionizing Radiation on Elementary Biological Objects. Hermann Dertinger , Horst Jung , R. P. O. Huber , P. A. Gresham', *The Quarterly Review of Biology*, vol. 46, no. 1, pp. 72–73, Mar. 1971, doi: 10.1086/406766.
[32] V. Arena, *Ionizing radiation and life; an introduction to radiation biology and biological radiotracer methods*. Saint Louis, Mosby, 1971.
[33] E. J. Hall and A. J. Giaccia, *Radiobiology for the Radiologist*. Wolters Kluwer Health, 2018.
[34] J. Bourhis *et al.*, 'Clinical translation of FLASH radiotherapy: Why and how?', *Radiotherapy and Oncology*, vol. 139, pp. 11–17, Oct. 2019, doi: 10.1016/j.radonc.2019.04.008.

[35] T. Prempree, A. Michelsen, and T. Merz, ‘The repair time of chromosome breaks induced by pulsed x-rays on ultra-high dose-rate’, *Int. J. Radiat. Biol. Relat. Stud. Phys. Chem. Med.*, vol. 15, no. 6, pp. 571–574, 1969, doi: 10.1080/09553006914550871.
[36] H. Weiss, E. R. Epp, J. M. Heslin, C. C. Ling, and A. Santomasso, ‘Oxygen Depletion in Cells Irradiated at Ultra-high Dose-rates and at Conventional Dose-rates’, *International Journal of Radiation Biology and Related Studies in Physics, Chemistry and Medicine*, vol. 26, no. 1, pp. 17–29, Jan. 1974, doi: 10.1080/09553007414550901.
[37] G. Pratx and D. S. Kapp, ‘Ultra-High-Dose-Rate FLASH Irradiation May Spare Hypoxic Stem Cell Niches in Normal Tissues’, *International Journal of Radiation Oncology*Biology*Physics*, vol. 105, no. 1, pp. 190–192, Sep. 2019, doi: 10.1016/j.ijrobp.2019.05.030.
[38] Y. Zhu, A. E. Dean, N. Horikoshi, C. Heer, D. R. Spitz, and D. Gius, ‘Emerging evidence for targeting mitochondrial metabolic dysfunction in cancer therapy’, *Journal of Clinical Investigation*, vol. 128, no. 9, pp. 3682–3691, Aug. 2018, doi: 10.1172/JCI120844.
[39] M. S. Alexander *et al.*, ‘Pharmacologic Ascorbate Reduces Radiation-Induced Normal Tissue Toxicity and Enhances Tumor Radiosensitization in Pancreatic Cancer’, *Cancer Res*, vol. 78, no. 24, pp. 6838–6851, Dec. 2018, doi: 10.1158/0008-5472.CAN-18-1680.
[40] N. Aykin-Burns, I. M. Ahmad, Y. Zhu, L. W. Oberley, and D. R. Spitz, ‘Increased levels of superoxide and H2O2 mediate the differential susceptibility of cancer cells versus normal cells to glucose deprivation’, *Biochem. J.*, vol. 418, no. 1, pp. 29–37, Feb. 2009, doi: 10.1042/BJ20081258.
[41] ‘43.O2·− and H2O2-Mediated Disruption of Fe Metabolism Causes the Differential Susceptibility of NSCLC and GBM Cancer Cells to Pharmacological Ascorbate.pdf’. .
[42] ‘47.Adapting the γ-H2AX Assay for Automated Processing in Human Lymphocytes. 1. Technological Aspects.pdf’. .
[43] H. C. Turner *et al.*, ‘Adapting the γ-H2AX Assay for Automated Processing in Human Lymphocytes. 1. Technological Aspects’, *Radiat Res*, vol. 175, no. 3, pp. 282–290, Mar. 2011, doi: 10.1667/RR2125.1.
[44] T. B. Kryston, A. B. Georgiev, P. Pissis, and A. G. Georgakilas, ‘Role of oxidative stress and DNA damage in human carcinogenesis’, *Mutation Research/Fundamental and Molecular Mechanisms of Mutagenesis*, vol. 711, no. 1, pp. 193–201, Jun. 2011, doi: 10.1016/j.mrfmmm.2010.12.016.
[45] D. De Ruysscher, E. Sterpin, K. Haustermans, and T. Depuydt, ‘Tumour Movement in Proton Therapy: Solutions and Remaining Questions: A Review’, *Cancers*, vol. 7, no. 3, pp. 1143–1153, Jun. 2015, doi: 10.3390/cancers7030829.
[46] S. van de Water, S. Safai, J. M. Schippers, D. C. Weber, and A. J. Lomax, ‘Towards FLASH proton therapy: the impact of treatment planning and machine characteristics on achievable dose rates’, *Acta Oncol*, vol. 58, no. 10, pp. 1463–1469, Oct. 2019, doi: 10.1080/0284186X.2019.1627416.
[47] P. van Marlen, M. Dahele, M. Folkerts, E. Abel, B. J. Slotman, and W. F. A. R. Verbakel, ‘Bringing FLASH to the Clinic: Treatment Planning Considerations for Ultrahigh Dose-Rate Proton Beams’, *International Journal of Radiation Oncology*Biology*Physics*, p. S0360301619340386, Nov. 2019, doi: 10.1016/j.ijrobp.2019.11.011.
[48] M.-C. Vozenin, J. H. Hendry, and C. L. Limoli, ‘Biological Benefits of Ultra-high Dose Rate FLASH Radiotherapy: Sleeping Beauty Awoken’, *Clinical Oncology*, vol. 31, no. 7, pp. 407–415, Jul. 2019, doi: 10.1016/j.clon.2019.04.001.
[49] P. P. Cruijsen, ‘First results on treatment planning with proton transmission beams to explore the potential of FLASH-PT for early stage lung cancer’, Erasmus medical centre, Rotterdam, The Netherlands, Internship report, Dec. 2019.
[50] A. Patriarca *et al.*, ‘Experimental Set-up for FLASH Proton Irradiation of Small Animals Using a Clinical System’, *International Journal of Radiation Oncology*Biology*Physics*, vol. 102, no. 3, pp. 619–626, Nov. 2018, doi: 10.1016/j.ijrobp.2018.06.403.
[51] J. Groen, ‘Development of FLASH proton therapy visualisation tools’, Erasmus medical centre, Rotterdam, The Netherlands, Internship report, Jan. 2020.

6 Appendix

A. FLASH models based on radiolytic oxygen depletion

A.1. Model for ultra-high dose-rates (> 100 Gy/s)

The relative decrease in radiosensitivity for very-high dose-rates is given by [21]:

$$\delta_{ROD} = \frac{OER(p_0)D_p - \int_0^{D_p} OER(P_0 - L_{ROD}D)dD}{OER(P_0)D_p}$$

where:
δ_{ROD} = relative decrease in radiosensitivity;
OER(x) = oxygen enhancement ratio at oxygen tension x;
p = oxygen tension;
D_p = prescriped dose;
L_{ROD} = radiolytic oxygen depletion rate;

A.2. Model for very-high dose-rates (> 10 Gy/s)

The relative decrease in radiosensitivity for very-high dose-rates is given by [21]:

$$\delta_{ROD} = \frac{OER(P_{SS}) - \frac{1}{T}\int_0^T OER\big(p(r,t)\big)dt}{OER(P_{SS})}$$

where:
δ_{ROD} = relative decrease in radiosensitivity;
OER(x) = oxygen enhancement ratio at oxygen tension x;
p_{SS} = steady state oxygen tension;
p(r,t) = oxygen tension;
r = distance from capillary;
t = time in seconds;

B. Beam characteristics overview

Model	Radiation type	Energy (MeV)	Dose delivered (Gy)	Irradiation time (ms)	Mean dose-rate (Gy/s)	Dose-rate within the pulse (Gy/s)	effect	Reference
Mice, lung fibrosis	electrons	4.5	16-30	< 267	60	> 180000	yes	[2]
Mice, brain	electrons	4.5, 6	10	0.0018 - 100000	0.1 -5600000 [1]	5600000	yes	[3]
Pig, skin	electrons	4.5, 6	22 - 34	< 113	300		yes	[4]
Cat,s nasal squamous cell carcinomas	Electrons	4.5, 6	25 - 41	< 137	300		yes	[4]
Mice, tumour	Photon	0.124	3.6-23.3	< 630	37-41		no	[27]
Mice brain	X-rays	0.102	10	270	37	12000	yes	[5]
Human,lung fibroblasts cells	Protons (singletron)	4.5	0-(20)	<200	100, 1000	100, 1000	yes[2]	[6]
Mice brain, zebrafish	electrons	6	10-14	<140	>100	>1800000	yes	[7]
Mice, Brain	Electrons	16,20	30	100 - 160	200,300	8750000	yes	[8]
Human skin tumour	electrons	5.6	15	90	167		yes	[9]
Zebrafish embryo	Protons (cyclotron)	224	0-42, 23	< 500	100	1000	no	[28]
Mice, intestine fibrosis and stem cell repopulation	Protons (cyclotron)	230	15	192	78		yes	[10]
Human, Prostate cancer cells	Electrons	10	18	30	600		yes	[11]
Mice, lung fibrosis	Electrons	4.5	5.2, 4, 17	<100	>52		yes	[12]
Mice, Intestine	Electrons	16	16,14	<80	216		yes	[13]

Calculated value

[1] FLASH found for dose-rates > 30 Gy/s.
[2] FLASH only found for 20 Gy and 1000 Gy/s.